OXFORD GENETICS

GENETICS, 2021, 217(4), iyab007
DOI: 10.1093/genetics/iyab007
Advance Access Publication Date: 23 January 2021
Investigation

New regulators of *Drosophila* eye development identified from temporal transcriptome changes

Manon Quiquand[1], Gerard Rimesso[1,†], Nan Qiao[2], Shengbao Suo[2], Chunyu Zhao[2], Matthew Slattery[3,‡], Kevin P. White[3,§], Jackie J. Han[2,¶], and Nicholas E. Baker [1,4,5,*]

[1]Department of Genetics, Albert Einstein College of Medicine, Bronx, NY 10461, USA
[2]CAS Key Laboratory of Computational Biology, CAS-MPG Partner Institute for Computational Biology, Shanghai Institute of Nutrition and Health, Chinese Academy of Sciences Center for Excellence in Molecular Cell Science, Collaborative Innovation Center for Genetics and Developmental Biology, Shanghai Institutes for Biological Sciences, Chinese Academy of Sciences, Shanghai 200031, China
[3]Institute for Genomics & Systems Biology, University of Chicago, Chicago, IL 60637, USA
[4]Department of Ophthalmology and Visual Sciences, Albert Einstein College of Medicine, Bronx, NY 10461, USA
[5]Department of Developmental and Molecular Biology, Albert Einstein College of Medicine, Bronx, NY 10461, USA
[†]Present address: TransViragen, Inc., P.O. Box 110301, Research Triangle Park, NC 27709, USA.
[‡]Present address: Department of Biomedical Sciences, University of Minnesota Medical School, 1035 University Drive, Duluth, MN 55812, USA.
[§]Present address: Tempus, 600 W Chicago Ave. Ste 510, Chicago, IL 60654, USA.
[¶¶]Present address: Peking-Tsinghua Center for Life Sciences, Academy for Advanced Interdisciplinary Studies, Center for Quantitative Biology (CQB), Peking University, Beijing 100871, China.

*Corresponding author: nicholas.baker@einsteinmed.org

Abstract

In the last larval instar, uncommitted progenitor cells in the *Drosophila* eye primordium start to adopt individual retinal cell fates, arrest their growth and proliferation, and initiate terminal differentiation into photoreceptor neurons and other retinal cell types. To explore the regulation of these processes, we have performed mRNA-Seq studies of the larval eye and antennal primordial at multiple developmental stages. A total of 10,893 fly genes were expressed during these stages and could be adaptively clustered into gene groups, some of whose expression increases or decreases in parallel with the cessation of proliferation and onset of differentiation. Using *in situ* hybridization of a sample of 98 genes to verify spatial and temporal expression patterns, we estimate that 534 genes or more are transcriptionally upregulated during retinal differentiation, and 1367 or more downregulated as progenitor cells differentiate. Each group of co-expressed genes is enriched for regulatory motifs recognized by co-expressed transcription factors, suggesting that they represent coherent transcriptional regulatory programs. Using available mutant strains, we describe novel roles for the transcription factors SoxNeuro (SoxN), H6-like homeobox (Hmx), CG10253, without children (woc), Structure specific recognition protein (Ssrp), and multisex combs (mxc).

Keywords: drosophila eye; eye differentiation; retinal differentiation; eye development; progenitor cell differentiation; terminal differentiation; developmental switch; transcriptome profile

Introduction

Neural development has been much studied in the *Drosophila* eye. Among other topics, these studies have made important contributions to the understanding of cell–cell interactions in development, of the function of proneural genes, of the neuronal recruitment by receptor tyrosine kinases, the mechanisms of lateral inhibition, the control of the cell cycle, and of cell death, of the choice of photoreceptor rhodopsin in color vision, and target selection by photoreceptor neurons(Cagan 2009; Treisman 2013; Viets *et al.* 2016; Baker 2017; Davis and Rebay 2017; Perry *et al.* 2017; Baker and Brown 2018; Kumar 2018). Multiple transcription factors have been discovered through functions in the *Drosophila* eye, including Eyeless (Ey), the *Drosophila* homolog of Pax6 (Quiring *et al.* 1994), Shaven (sv), the *Drosophila* homolog of Pax2 (Fu and Noll 1997), and wSine Oculis (so), the founder of the Six family of homeodomain proteins (Kawakami *et al.* 2000).

Differentiation starts in the eye disc about 72 h after egg laying (AEL), early in the third larval instar, when the morphogenetic furrow (MF) is established (Figure 1, A–D). The MF is a transient indentation that moves across the eye imaginal disc epithelium from posterior to anterior, as the retinal progenitor cells cease growth and begin to acquire specific fates and differentiate (Wolff and Ready 1993; Roignant and Treisman 2009). Ahead of the MF, undifferentiated cells proliferate asynchronously. Posterior to the MF, cells differentiate and organize into columns of ommatidia (unit eyes of the adult compound eye). The first ommatidial cell fate is that of R8 photoreceptor cells, determined in the MF by the proneural transcription factor Atonal (Ato), followed by the EGFR-dependent recruitment of other photoreceptor cell types. About 30 columns of ommatidia have begun differentiation by ~132 h AEL when the larva pupariates (Wolff and Ready 1993; Roignant and Treisman 2009).

Received: March 15, 2020. **Accepted:** December 28, 2020

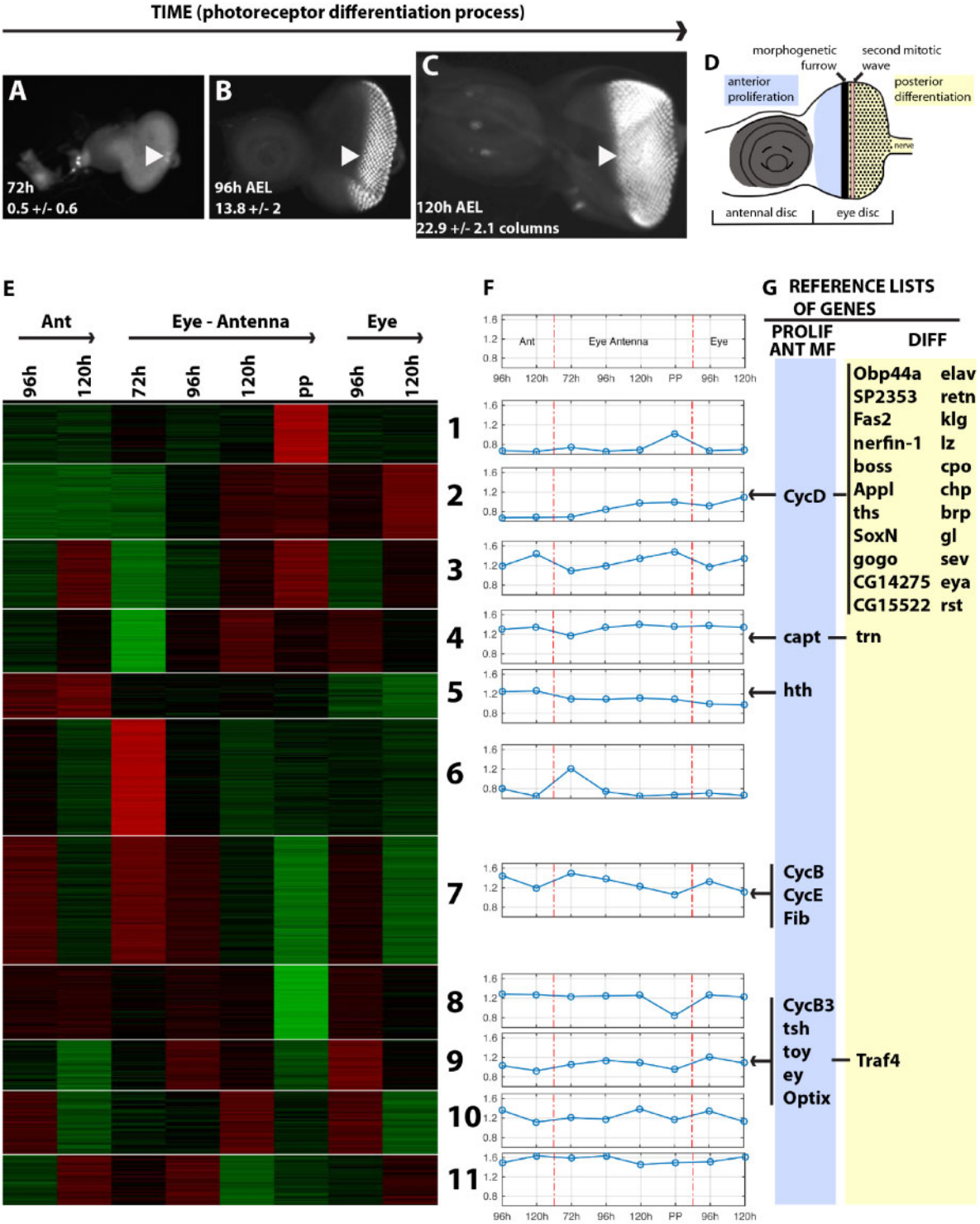

Figure 1 Temporally regulated transcription during *Drosophila* eye development. (A–C) Eye imaginal discs from 72 to 120 h after egg laying (AEL) labeled with ELAV to monitor the differentiated photoreceptors appearance posterior to the morphogenetic furrow (MF) (arrowhead). Anterior side is shown to the left. During the third larval instar the eye imaginal disc grows and the MF progresses from the posterior margin toward the anterior, associated with a wave of differentiation. (A) 72-h AEL, the first photoreceptors differentiate. On average of 0.5 ± 0.6 columns of ommatidia were differentiated at this stage. (B–C) 96 h AEL and 120 h AEL. 13.8 ± 2 and 22.9 ±2.1 columns of ommatidia, respectively. (D) Cartoon of the eye antennal imaginal disc with anterior to the left, indicating the location of generally proliferating cells anterior to the morphogenetic furrow (MF) in blue and differentiating cells posterior to the MF in yellow. Also indicated is the approximate location of the Second Mitotic Wave. (E) BIC-SK means supervised adaptative clustering of the RNA-sequencing data including 8 eye and/or antenna disc samples at different time points. 10893 genes were expressed with an FPKM ≥ 0.5 in at least one of the 8 RNA samples. The expression level of each gene is normalized and indicated by color (red=high, green = low). Eleven clusters of related transcription profiles best represented this data. (F) Mean expression levels for each of the 11 expression clusters. Differentiation genes have to be activated posterior to the MF and their expression levels should increase over time. Progenitor genes should be inactivated posterior to the MF and their expression levels should decrease over time. (G) Distribution of well-established reference genes among the gene-expression clusters. Differentiation genes were concentrated in cluster 2, which shows expression increasing with time in eye and in eye-antenna, but not in antenna. Progenitor genes were most common in clusters 7 and 9, which both featured decreasing expression in eye discs and antenna discs.

Hedgehog (Hh) and Decapentaplegic (Dpp) signals, along with a contribution from Notch, act together to drive the MF across the eye imaginal disc. These signals act through the transcription factors Cubitus Interruptus (Ci), Mothers Against Dpp (Mad) and Suppressor of Hairless (Su(H)), respectively (Greenwood and Struhl 1999; Curtiss and Mlodzik 2000; Baonza and Freeman 2001; Li and Baker 2001; Fu and Baker 2003). Posterior to the MF, receptor tyrosine kinases signal through the Ras pathway, targeting the Ets-domain transcription factors Pointed (Pnt) and Anterior-Open(Aop)/Yan(Nagaraj and Banerjee 2004; Roignant and Treisman 2009). These signaling pathways are also active in other tissues and it is thought that the retinal determination genes (*ey*, *teashirt* (*tsh*), *eyes absent* (*eya*), *dachshund* (*dac*), and *so*) act combinatorially with these signals to regulate the specific expression of eye gene targets (Curtiss *et al.* 2002; Mann and Carroll 2002; Baker and Firth 2011; Treisman 2013; Pichaud 2014; Davis and Rebay 2017). Retinal determination genes, *i.e.*, genes capable of inducing ectopic eye differentiation when expressed in other tissues, encode transcriptional regulators that are coordinately expressed during eye development(Davis and Rebay 2017). Ey and Tsh, along with a cofactor Homothorax (Hth), are expressed in proliferating progenitor cells, disappearing as differentiation starts, whereas Eya, So and Dac turn on to replace them as the MF approaches(Bessa *et al.* 2002; Firth and Baker 2009).

How target genes are transcribed to achieve eye differentiation has not been completely described. SAGE, microarray, and RNA-Seq studies have identified gene expression specific to retinal differentiation, either through comparison to other tissues, or through covariation of gene expression (Jasper *et al.* 2002; Aerts *et al.* 2010; Potier *et al.* 2014). Target genes have been identified with various degrees of validation for the eye-specific transcription factor Glass (Gl), for the proneural bHLH transcription factor Ato that defines the founder photoreceptor R8, and the retinal determination gene proteins So and Eya (Hayashi *et al.* 2008; Aerts *et al.* 2010; Naval-Sanchez *et al.* 2013; Jusiak *et al.* 2014a, 2014b; Bernardo-Garcia *et al.* 2016; Jin *et al.* 2016; Liang *et al.* 2016; Morrison *et al.* 2018). This leaves many aspects of eye differentiation poorly understood, for example, few of the identified target genes seem to be the terminal effectors directly determining the properties of differentiated cells, possibly because their mutants do not always show externally visible phenotypes, and less is known about genes that are down-regulated with differentiation.

In addition to differentiation into terminal cell types, further properties distinguish the cells of the posterior retina from the unspecified progenitor cells anterior to the MF. Differentiating cells undergo a terminal cell cycle arrest, contrasting with the earlier proliferation of the uncommitted cells. Terminal cell cycle withdrawal is mediated in part by the uncoupling of Cyclin E/Cdk2 activity from transcriptional activity of E2F1, breaking a positive feedback loop that is active in proliferating cell populations (Firth and Baker 2005; Buttitta *et al.* 2007; Ruggiero *et al.* 2012). Cell cycle quiescence is accompanied by changes in the nucleolus, suggested to reflect reduced ribosome biogenesis accompanying the reduced growth requirement of non-proliferating cells. The basis for these growth changes is not known but may reflect transcriptional changes as they depend on part on the transcription factors Mad and Ci (Baker 2013). Changes in many aspects of metabolism might be expected to accompany these growth changes, but have not been identified in the *Drosophila* eye (Tu *et al.* 2005).

Changes in signal transduction pathways also occur. The Hh pathway provides an example. Anterior to the MF, and in most other tissues, Hh modulates the Cullin1-dependent processing of Ci into a transcriptional repressor. Posterior to the MF, the F-box protein Roadkill (Rdx) instead promotes the Cullin3-dependent complete degradation of Ci, thereby desensitizing cells behind the furrow to Hh signaling (Ou *et al.* 2002; Kent *et al.* 2006; Zhang *et al.* 2006). It is speculated that Dpp signaling mechanisms may differ posterior to the MF also, as part of a mechanism that keeps the MF moving forwards (Lim and Choi 2004; Baker *et al.* 2009).

It is an intriguing possibility that changes in differentiation, signaling, growth, and the cell-cycle that accompany eye development might be coordinated by transcriptional regulation that would particularly distinguish the differentiating retina posterior to the MF from the undifferentiated progenitor cells anterior to the MF. In this study, we attempted to identify these gene sets by classifying genes into distinct gene expression networks according to similarity of temporal expression profile. Since the MF moves across the eye, taking about 60 h to convert all the proliferating progenitor cells into terminally differentiating retina, we hypothesized that genes transcribed during retinal differentiation would represent an increased fraction of the transcriptome with time, as the differentiating region comprised more of the eye disc. Conversely, genes transcribed in proliferating progenitor cells might be expected to decrease over time. Accordingly, we used mRNA-Seq to characterize gene expression changes in eye-antennal discs over time, from the mid-third larval instar (72 h AEL) until the onset of pupariation (about 130 h AEL in our experiments), hypothesizing that temporal changes in gene expression levels might be sufficient to identify genes whose expression changes with the onset of differentiation. Because gene expression might also change temporally in these complex tissue samples for other reasons, we used an unsupervised clustering approach to define the main temporal gene expression programs occurring in the eye-antennal imaginal discs in an unbiased manner. This approach identified large sets of genes both up- and down-regulated concomitant with the start of differentiation, and several genes with mutant phenotypes affecting either eye growth or differentiation.

Materials and methods

RNA isolation, cDNA synthesis, and RNAseq

Drosophila adults (w^{11-18} strain) were allowed to lay eggs on yeast-glucose media for 2 h and samples prepared at the indicated times. RNA samples were prepared in Trizol as described previously (Firth and Baker 2007). This results in RNA extraction from living larvae within minutes, unlike tissue dissociation and FACS sorting, for example. PolyA RNAs were purified using the MicropolyA Purist Kit from Ambion and converted into single-stranded DNA after Reverse Transcription using random hexamers. The second strand synthesis was carried out by adding to the reaction RNase H (Invitrogen #18021014) and DNA Polymerase II (NEB #M0209S). At this stage, the double-stranded DNA was cleaned up on Qiagen Quiaquick columns and the ends were repaired using the T4DNA Polymerase, Klenow Fragment, and T4 PNK enzymes. After another round of Qiaquick purification, an A residue was added with Klenow [3'>5' exo-] enzyme and the product was again purified on Quiaquick columns. Adapters from Illumina for LM-PCR were then ligated to the end of the DNA molecules. The product of the reaction was run on an Agarose gel (2% NuSieve) and a band corresponding to 300 bp was then extracted and purified. 20 cycles of PCR reaction were then performed using phusion polymerase (Finnzyme F-530S) and the Illumina oligos. The product was purified by gel electrophoresis. Illumina sequencing was then performed on a Genome Analyzer

II. Primary mRNA Seq data are available from the GEO under accession number GSE164079.

Pre-processing of RNA-seq data

The quality of raw sequencing reads was evaluated by the FASTQC. Short read quality assessment was performed by Genome Analyzer on RNA-seq samples at the different time points. GC content, read distribution and read quality were all sufficient for further computational analysis. Then RNA-seq reads were mapped to dm3 version of the Drosophila genome using Tophat (Kim *et al.* 2013) with the default parameters. Most samples had nearly 70 milion total reads with mapping ratio after filtering ~70-80% (Supplementary Table S15). The mapped reads were then fed to Cufflinks (Trapnell *et al.* 2013) to quantify gene expression levels (fragment per kilobase per million, FPKM) with the default parameters. Genes with the FPKM >0.5 in at least one sample were selected for further analysis. Finally, the expression levels were transformed to logarithmic space using $\log_{10}(\text{FPKM}+1)$.

BIC-SK means clustering analysis

To determine the optimal number of gene clusters, an adaptive clustering algorithm based on the Bayesian Information Criterion (BIC) was used, and then followed with deep clustering by using unsupervised super k-means algorithm (BIC-SKmeans) (Zhang *et al.* 2013). Samples were ordered based on the development stages. Before clustering, we used the z-score to normalize gene expression levels across all samples. For genes in clusters 2, 7, and 9, we also used BIC-SKmeans clustering again to get more detailed sub-clusters.

Functional enrichment analysis

Gene Ontology (GO) and Kyoto Encyclopedia of Genes and Genomes (KEGG) pathways enrichment analyses were performed with script findGO.pl in Homer software (Heinz *et al.* 2010) for each gene cluster. FDR was calculated by Benjamini Hochberg (BH) multiple testing correction based on *P*-values.

Cis-regulatory feature analysis

We used two methods to perform motifs/TFs enrichment analysis based on promoter sequences of a gene list: (1) the query gene list was uploaded to i-*cis*Target (https://gbiomed.kuleuven.be/apps/lcb/i-cisTarget/) (Imrichová *et al.* 2015) to identify enriched motifs/TFs within genes and 5 kb upstream with the default parameters (*Drosophila melanogaster* (dm3) was selected), with significance cutoff (Normalized Enrichment Score >3); (2) As well as using the motifs contained in Homer, we also downloaded motifs from Fly Factor Survey (http://mccb.umassmed.edu/ffs/DownloadData.php). Then findMotifs.pl script from Homer was used to identify enriched motifs/TFs with the following parameter: "fly -start -1000 -end 500 -len 4,6,8,10,12". Briefly, for a gene list of interest, this searches for motifs of length 4, 6, 8, 10 or 12 bp that are enriched within the sequences from 1 kb upstream of the transcription start site to 500 bp downstream of the transcription termination site, in comparison to other genes (Heinz *et al.* 2010). We used the same iCis and Homer strategies to perform motifs/TFs enrichment analysis for sub-clusters.

In some cases, multiple transcription factors were candidates to bind the same site. For example, cluster 2 genes were enriched for two E-box sequences that may be recognized by any of 10 bHLH proteins. Of those, *ato* and *daughterless* (da) have known functions in larval eye disc differentiation (Jarman *et al.* 1994; Brown *et al.* 1996). Many of the other bHLH proteins have roles in neurogenesis in the antennal disc (as well as in other processes in other tissues such as myogenesis) (Baker and Brown 2018). Accordingly, lists of potential transcription factors could include some that are not involved in the expression of cluster 2 genes, but with similar binding sites.

Riboprobes synthesis, in situ hybridization

Digoxigenin-labeled RNA probes were synthesized as described (Firth and Baker 2007) and resuspended in 50ul of DEPC-water. The primer sequences are reported in Supplementary Table S6. Most of the PCR products (92/98) used to amplify riboprobes were between 400 and 600 base pairs. *In situ* hybridization (ISH) was performed after (Cornell, 1999) on *Drosophila* eye discs (around 10 pairs per probes) in 2 ml ependorf tubes, after fixation with 4% formaldehyde (FA) in phosphate-buffered saline (PBS) for 20-30 min at room temperature. Samples were rinsed in PBS before storage in 100% methanol at -20°C until use. Before hybridization, eye discs were rehydrated in methanol/PBS-Tw (0.1% tween 20) 7:3 and 3:7, transferred to PBS-Tw for 5 min each on moving platform, fixed in 4% FA/PBS 5 min at room temperature. Samples were then rinsed 2 times in PBS-Tw, washed 3 times for 10 min in PBS-Tw on moving platform, washed in PBS-Tw/HSW (50% formamide, 5X SSC, 0.07 M citric acid, 0.1% Tween 20) 1:1 10 min on moving platform and washed in HS (50% formamide, 5X SSC, 0.07 M citric acid, 0.1% Tween 20, 100ug/ml tRNA, 50ug/ml heparin) for 10 min. Prehybridization was performed for 1 h at 65°C in HS and hybridization overnight at 65°C in HS with riboprobes, which have been denaturated at 80°C for 10 min in 20ul of HS. Then eye discs were rinsed at 65°C in prewarmed HSW, washed 2 times 20 min at 65°C in HSW, washed for 20 min in PBS-Tw/HSW 1:1 at 65°C, rinsed 2 times in PBS-Tw at room temperature, washed 2 times 30 min at room temperature in PBS-Tw on moving platform. Samples were incubated with an alkaline phosphatase-conjugated anti-digoxigenin antibody at 1/2000 in PBS-Tw for 1.5 h, rinsed 2 times in PBS-Tw and washed 5 times 10 min in PBS-Tw on moving platform. After incubation of the samples in NMTT (0.1 M NaCl, 0.05 M MgCl2, 0.1 M TrisCl pH9.5, 0.1% Tween-20) 2 times for 5 minutes, the conjugated antibody was detected using NBT/BCIP in NMTT for desired length of time.

Fly strains and genetic manipulations

Drosophila was raised at 25°C on standard cornmeal agar except where indicated otherwise. Mosaic mutant clones were generated by flippase-mediated mitotic recombination technique with an eyeless-flippase (eyFLP) induction (Newsome *et al.* 2000). Homozygous mutant cells were identified on eye disc by the absence of GFP staining (corresponding to the absence of arm-lacZ or GFP) and on adult eye by their dark red color for *CG10253* and *Ssrp* or white color for *woc*. In order to examine adult eyes of almost only homozygous mutant cells, mitotic clones were generated in a Minute background. *Drosophila* mutant strains were obtained from Bloomington and recombined with linked FRT sites. The following alleles were used: $SoxN^{NC14}$, $Hmx^{MI02025}$, $CG10253^{f02060}$, woc^{251}, $Ssrp^{G2947}$, $CG15514^{EP1005}$, crp^{k00809}. *mxc* ^{XM20C} allele recombined with FRT19A was kindly provided by H. Bellen's laboratory (Yamamoto, 2014).

Marked, Minute chromosomes used included: [*armLacZ*] FRT40, FRT82 M95c [*armLacZ*] Gal80, FRT82 [*armLacZ*], FRT42 M56i [*armLacZ*], FRT42, FRT42D *UbiGFP*, *armLacZ*11:3 FRT19A, M [*armLacZ*] FRT40. The ey-Gal4 line was that of (Hazelett *et al.* 1998).

Transgenic RNAi lines were obtained from VDRC or the transgenic RNAi project (TRiP) (for details see Supplementary Table S11). Driver strains used for RNAi screen included: UAS dcr2 *glass lacZ*/CyO;; *eyeless-Gal4* (kindly provided by J. Treissman's

laboratory) and w; *GMR-Gal4*, *UAS-Dcr2*/CyO; Sb/TM6B. Cultures were grown at 29°C to assess RNAi phenotypes.

Immunofluorescence

Immunofluorescence was performed as described in (Baker, 2014). The following primary antibodies were used: rabbit anti-beta gal (1/20, Cappel), rabbit anti-GFP (1/50, Invitrogen), rat anti-ELAV (1/50, DSHB 7E8A10), mouse anti-Cut (1/20, DSHB 2B10), mouse anti-discs large (1/500, DSHB, 4F3). Secondary antibodies conjugated with Cy2, Cy3, and Cy5 dyes (1:200) were from Jackson ImmunoResearch Laboratories.

Preparations were pictured on the Leica SP2 confocal microscope. Images were processed using Image J64 and Adobe Photoshop CS3 software.

Data availability

Strains and plasmids are available upon request. Supplementary tables are available at Figshare through the GSA portal (https://doi.org/10.25386/genetics.13394135). RNA-Seq raw data will be available through GEO. The authors affirm that all other data necessary for confirming the conclusions of the article are present within the article, figures, and tables.

Results

Gene transcription profile during *Drosophila* eye morphogenesis

RNAs were extracted from the eye-antennal primordium at four time points: at the larval stage 72 h, 96 h, or 120 h AEL and at the white prepupal stages (about 130 h AEL in our experiments) (Figure 1, A–D). At 96 and 120 h AEL it was also possible to dissect the eye and antenna discs apart for separate analysis. At 72 h AEL eye-antennal discs were initially dissected along with the attached mouth-hook structures, in case we were unable to recover sufficient material from these small eye-antennal discs alone, but also then as eye-antennal imaginal discs alone. Finally, RNAs were also extracted from whole larvae at 72, 96, 120 h AEL (Supplementary Figure S1A).

Supplementary Table S1 summarizes mRNA abundance from these 12 samples, as Fragments per Kilobase per Million (FPKM). Supplementary Figure S1B shows unsupervised clustering of gene expression levels from these 12 RNA samples. RNAs from the whole animal samples were more closely related to one another than to any of the samples from imaginal discs, perhaps because the larval body contains many tissue types such as skeletal muscle, gonad, intestine, central nervous system, etc., that are not present in the imaginal discs. Within the imaginal disc samples, eye-antennal discs were more similar to eye discs than to antennal discs, suggesting that eye tissue provides the majority of transcriptional changes, and white-prepupal eye-antennal discs were more different from the other samples.

We first performed unsupervised clustering of genes according to similarity of temporal gene expression profile, without assumptions about which samples should be enriched for progenitor or differentiation genes. We used Bayesian Adaptive Clustering with the super k-means algorithm (BIC-SK means), which also optimizes the number of gene expression clusters (Zhang *et al.* 2013). As noted above, the whole larva sequences were very distinct and clustering at first separated genes primarily according to those expressed in whole larvae and genes that were not (Supplementary Figure S1C). Thus although the whole larva sequences had been included to augment the data available for clustering, this proved unhelpful, and subsequent analyses were restricted to the 8 samples derived only from imaginal disc tissues, which proved sufficient for effective clustering, in order to focus on transcription programs within the imaginal discs. Using FPKM > 0.5 as a threshold, 10,893 genes were expressed in the imaginal disc samples, representing 78% of the *Drosophila* coding genes, and 83% of the genes for which expression (FPKM > 0.5) was detected in any of the samples (*i.e.*, including whole larvae). BIC-SK means indicated that the optimum cluster number to best represent these data was 11, indicating that gene expression in eye-antennal imaginal discs was best described by 11 programs of gene expression (Figure 1E; Supplementary Figure S2). The genes in each of the 11 clusters are listed in Supplementary Table S2 and the mean changes in gene expression across the different samples are summarized for each cluster in Figure 1F.

A cluster of retinal differentiation genes with an expression profile increasing with time

To help identify gene expression associated with eye differentiation without assuming its temporal gene expression profile, a set of 24 well-characterized genes whose transcription pattern has been unequivocally mapped posterior to the MF was collated. Many of these genes have known roles in eye patterning and differentiation (Supplementary Table S3). 22 of these 24 genes were found within gene transcription cluster 2 (Figure 1G). Cluster 2 contained 1029 genes and was characterized by transcript levels generally increasing over time in eye-antennal discs and in eye discs, but changing little in antennal discs (Figure 1F). Thus, the average expression profile of cluster 2 agreed with the hypothesis that retinal differentiation gene expression would increase over time. The most similar program of gene expression was seen in cluster 3, which differed in that expression levels also increased with time in antennal discs (Figure 1F). None of the 24 reference-gene set was recovered in cluster 3. Regarding the two reference genes not found in Cluster 2, *TNF-Associated Factor 4* (*Traf 4*) expression levels decreased from 96 h AEL to white prepupae in eye-antennal and eye disc samples, and accordingly *Traf4* was recovered in cluster 9 (Table 2 and Figure 1G). *Tartan* (*trn*) expression levels increased over time in eye-antennal and antennal discs, but decreased from 96 h-120h AEL in eye disc samples, and accordingly *trn* was recovered in cluster 4 (Table 2 and Figure 1G). These two examples illustrate that some genes expressed posterior to the MF [verified independently by two groups for *trn* (Firth and Baker 2007; Mao *et al.* 2008)] may nevertheless have other temporal expression profiles, possibly because of changing expression in the antennal region, or because of other temporal regulation superceding that due to progression of the MF. We also know that genes expressed in glial cells or hemocytes can be present in eye-antenna disc RNA samples (Firth and Baker 2007). Because ~90% of the reference differentiation gene set were recovered in cluster 2, however, cluster 2 is predicted to contain many genes that turn on posterior to the MF.

Cluster 2 was statistically enriched for 227 biological process GO terms (FDR_BH $P < 0.01$: Supplementary Table S4), either explicitly associated with neurogenesis [*e.g.*, neurogenesis (17), synaptogenesis (20), axogenesis (14), stimulus (8)] or otherwise consistent with eye development [*e.g.*, behavior (20), signaling (17), adhesion (8), transport (12), secretion (5), signaling pathways (4), etc.]. The top five GO terms were: generation of neurons, neuron differentiation, biological regulation, neuron development, regulation of cellular process. The five statistically enriched Kyoto Encyclopedia of 798 Genes and Genomes (KEGG) pathway terms (Enrichment $P < 0.01$) were phosphatidylinositol signaling

system, MAPK signaling pathway—fly, Jak-STAT signaling pathway, dorso-ventral axis formation, Inositol phosphate metabolism (Supplementary Table S5), some of which have known roles in eye differentiation (Rubin *et al.* 1997; Avet-Rochex *et al.* 2014; Tee *et al.* 2016; Vollmer *et al.* 2017). These enrichments are consistent with retinal differentiation roles for the gene expression profile represented by cluster 2.

At least half of the cluster 2 genes are transcribed posterior to the MF

The transcription pattern of a sample of 52 cluster 2 genes was explored by ISH to eye-antennal imaginal discs from third-instar larvae. Because genes expressed at low level might not be detected by ISH, only genes with transcript levels estimated by mRNA-Seq to be FPKM ≥ 3 in an eye-antenna or eye disc sample were tested. FPKM $= 3$ corresponded to the expression level of *bride of sevenless* (*boss*), which was the gene with the lowest expression successfully detected in pilot experiments (Figure 2A). Examples of these expression patterns are shown in Figure 2, B–J and the complete set is shown in Supplementary Figure S3 and summarized in Supplementary Table S6. 27/52 genes (52%) showed elevated transcription in the posterior, differentiating retina, whereas only seven showed other patterns (13%) (Supplementary Figure S3A). No specific transcription pattern could be discerned for 18/52 genes (35%) (Supplementary Figure S3B). In these latter cases it is difficult to distinguish uniform transcription (which may nevertheless increase over time) from failure to detect specific signal by ISH, either for technical reasons or because of low expression level on a per cell basis, so it remains uncertain whether these genes are expressed more highly posterior to the furrow or not. Because we never observed an expression pattern posterior to the MF among the control sense strand *in situs* (performed for 12 different genes) (Supplementary Table S6), such *in situ* signals are likely to be specific.

One of the seven genes classified as showing another pattern, *Enhancer of split mδ* (*E(spl)mδ*, aka *HLHmdelta*) was nevertheless associated with retinal differentiation (Supplementary Figure S3B). In addition to *E(spl)mδ* transcription posterior to the MF, strong transcription occurred at the anterior edge of the MF, where E(spl)mδ protein plays a role in Notch signaling during early eye patterning (Baker *et al.* 1996; Dokucu *et al.* 1996). Thus cluster 2 gene expression signature can include genes that are upregulated early in the differentiation process, before the MF arrives.

Because transcription of some cluster 2 genes was not elevated posterior to the furrow (*e.g.*, Figure 2F), a further Bayesian adaptive clustering was performed on just the 1029 cluster 2 genes alone, to see whether any substructure was detectable. This indicated that cluster 2 could itself be represented as two subclusters, cluster 2 A and cluster 2B (Figure 3; Supplementary Table S7). Cluster 2 A (779 genes) contained 21 of the 22 reference eye genes found within cluster 2, and 26 of the 27 other genes shown to be expressed behind the furrow by ISH experiments described above (Supplementary Table S6). Cluster 2 A was enriched for very similar GO terms to the parent cluster 2, and the same KEGG terms (Supplementary Tables S8 and S9). By contrast, cluster 2B (250 genes) contained 3 of the 7 cluster 2 genes expressed elsewhere than behind the furrow, and 3 genes for which the transcription pattern could not be determined (Supplementary Tables S6 and S7). No GO terms were significantly enriched and the only enriched KEGG term was 'ribosomes, eukaryotic', with the cluster2B containing four ribosomal protein genes *RpS10a*, *RpS12*, *RpS19b*, and *RpS9* (Supplementary Tables S8 and S9). Subclusters 2A and 2B show similar gene expression profiles to the parent cluster 2 except that for cluster 2B average gene expression increased in eye and eye-antennal discs from 72-120 h only and decreased between 120 h and the white prepupal stage (Figure 3). We conclude that cluster 2A is most highly enriched for the genes expressed posterior to the MF, although at least a few such genes exemplified by *Ca-beta* are found in cluster 2B.

A cluster of putative proliferation genes with expression profiles decreasing with time

Concomitant with the induction of eye differentiation genes posterior to the MF, genes associated with the proliferating progenitor cells anterior to the MF might be downregulated. We identified 11 'progenitor or proliferation' reference genes that had already been characterized for their expression anterior to the MF or in dividing cells (Supplementary Table S3). 8/11 were concentrated in two gene expression clusters, cluster 7 and cluster 9,

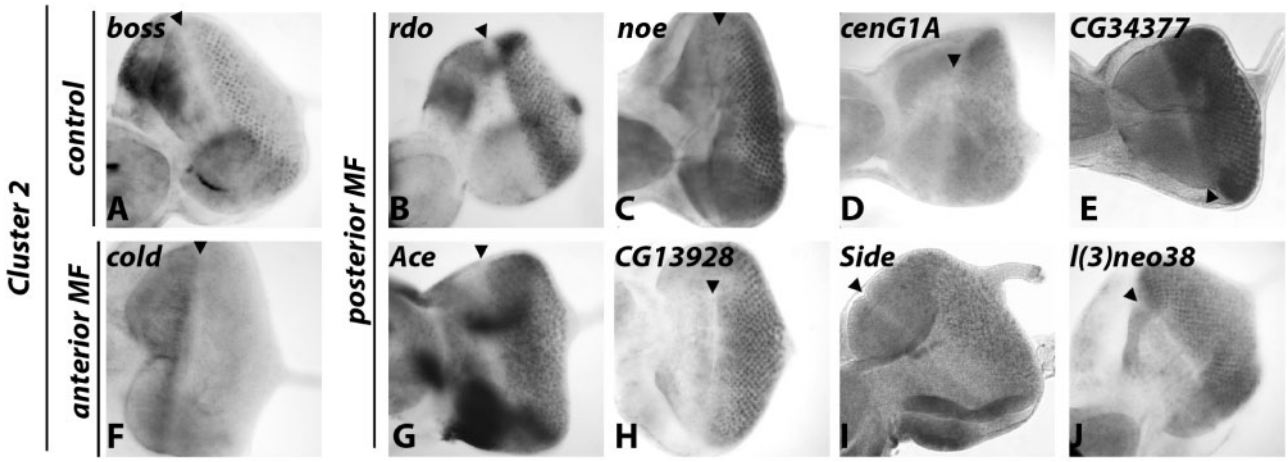

Figure 2 ISH detects transcription behind the furrow. ISH was performed on eye-antennal imaginal discs from third-instar larvae. Anterior side is shown to the left. ISH for boss (A), one of the reference genes known to be expressed posterior to the MF, and the transcript with the lowest FPKM detected in preliminary ISH experiments, shows expression in the single R8 precursor cells of each ommatidium. ISH verifies transcription of 52% of the genes included in the eye-specific differentiation cluster 2 in the posterior, differentiating retina eg panels (B–E, G-J). 13% of cluster 2 genes reveal other transcription patterns eg *cold* (F).

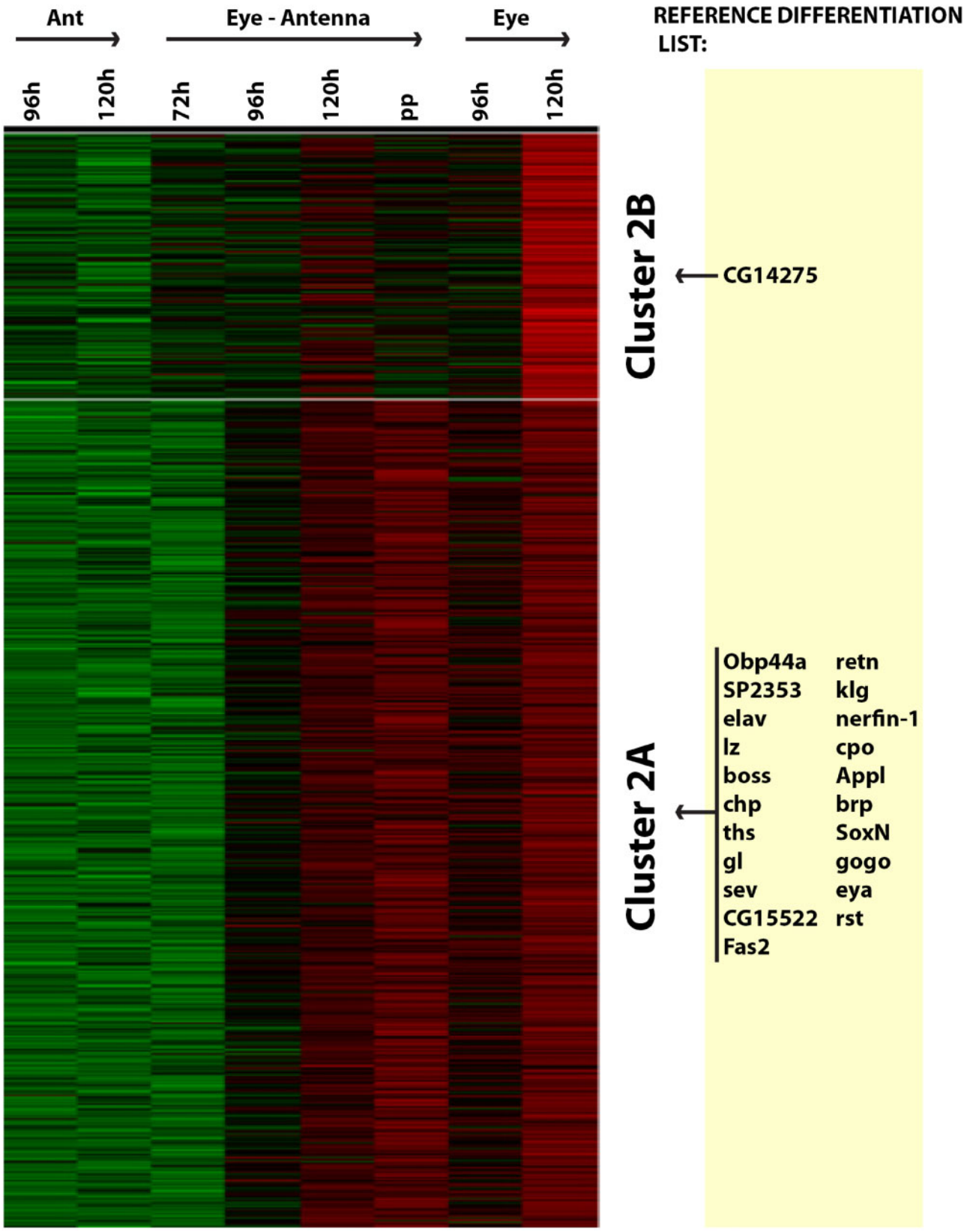

Figure 3 Subclustering of the differentiation genes. BIC-SK means supervised adaptative clustering of the RNA-sequencing data from 8 eye and/or antenna disc samples of cluster 2 only (1029 genes). Cluster 2 was subdivided into **c**lusters 2A (779 genes) and 2B (250 genes). Cluster 2A genes show the more pronounced temporal increase in transcription in the eye disc and contain most of the differentiating eye reference genes. ISH experiments like those shown in Figure 2 estimate that 58% of the genes included in the eye-specific differentiation cluster 2A are expressed posterior to the MF. The gene *cold*, which exemplified a cluster 2 gene with a different expression pattern (see Figure 2J), was found within cluster 2B.

suggesting that these might include genes downregulated as proliferation ceases and differentiation begins (Figure 1, F–G).

Cluster 7 (1753 genes) was characterized by gene expression generally decreasing over time in eye-antennal discs, eye discs, and antennal discs. The reference genes included in cluster 7 were *cyclin B* (*cycB*), *cyclin E* (*cycE*), and *fibrillarin* (*fib*). Cluster 7 was statistically enriched for 209 GO terms, 46% of them related to cell cycle, proliferation and growth (Supplementary Table S4). The top 5 GO terms were: cellular nitrogen compound metabolic process, nucleobase-containing compound metabolic process, heterocycle metabolic process, organic cyclic compound metabolic process, nitrogen compound metabolic process. All these are related to DNA synthesis. The 11 statistically enriched KEGG pathways include DNA replication, eukaryotic Ribosome biogenesis, mismatch repair, pyrimidine metabolism, nucleotide excision repair, BRCA1-associated genome surveillance complex, MCM complex, nuclear pore complex, homologous recombination, and base excision repair (Supplementary Table S5). All these are associated with DNA replication and maintenance, or with growth, consistent with the notion that cluster 7 is enriched for genes expressed in growing, proliferating cells.

The transcription pattern of genes from cluster 7 was explored by ISH to eye-antennal imaginal discs from third-instar larvae (Figure 4 and Supplementary Figure S4). ISH with probes for 21 genes from cluster 7 identified 6 genes with a 'cell cycle' pattern of transcription, in which expression was detected both anterior to the MF and in a band just posterior to the furrow corresponding to the position of the Second Mitotic Wave (SMW) cell cycle (*e.g.*, Figure 4, B–D). This pattern of transcription is typical for cell cycle genes such as *string/Cdk25* (*stg*), itself a member of Cluster 9 (Figure 4A). Probes for another 14 genes detected signals anterior to the MF, but not in the SMW (*e.g.*, Figure 4, E–G). For some of these probes an *in situ* signal was only seen in some of the discs hybridized. Because we have sometimes seen

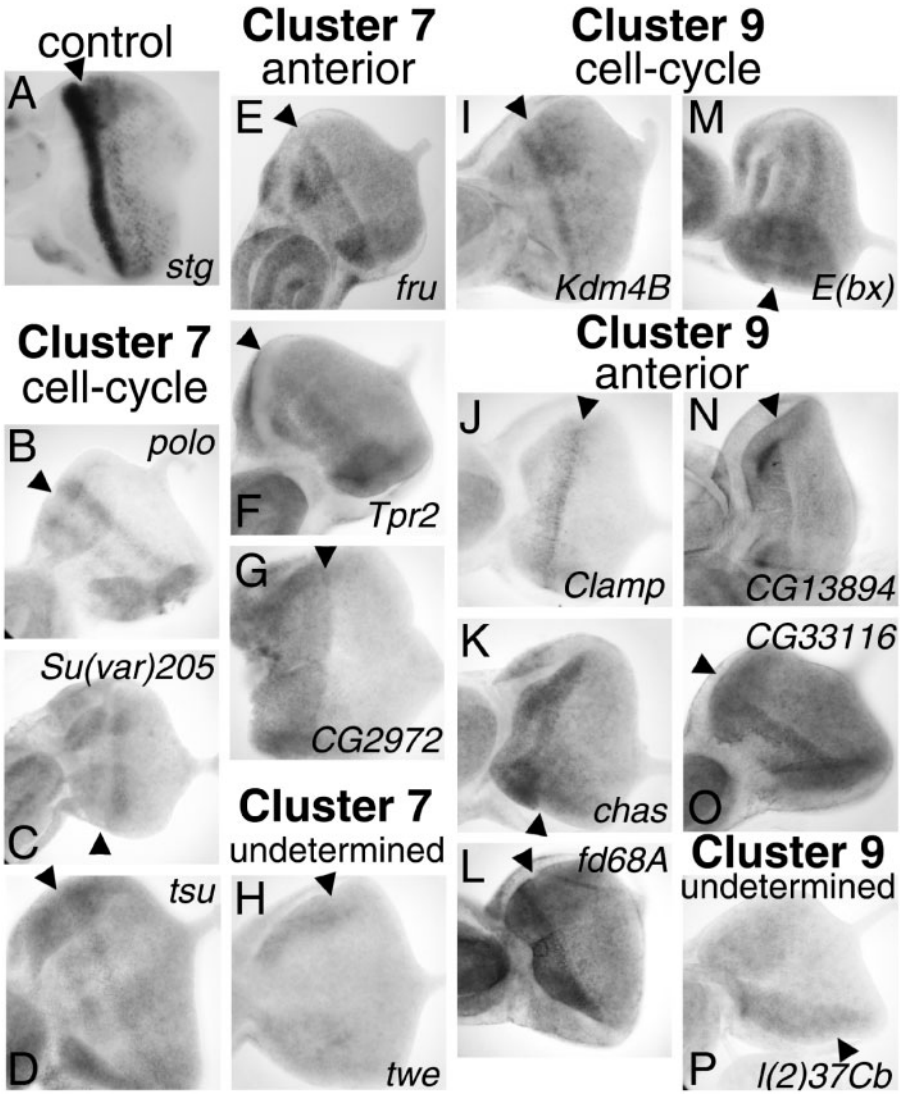

Figure 4 ISH detects transcription anterior to the furrow. ISH was performed on eye-antennal imaginal discs from third-instar larvae. Anterior side is shown to the left. ISH for string (Figure 4A) was used as a technical control because of its transcription both anterior to the MF and, at a lower level, in the second mitotic wave just posterior to the MF. The string gene is found in expression cluster 9. 2% of genes from cluster 7 were expressed in cell cycle patterns (e.g., B–D) or anterior to the MF (E–G). For other cluster 7 genes, no clear pattern of transcription was evident. 40% of genes from cluster 9 expressed in cell cycle patterns (I,M) or anterior to the MF (J–L, N–O). For other cluster 9 genes, no clear pattern of transcription was evident (P). The expression pattern pictures of all the 21 and 25 genes examined in the cluster 7 and 9, respectively, are available in Supplementary Figures S7 and S8.

sporadic anterior labeling with sense probes, we think it possible that such staining may sometimes represent a staining artifact. Therefore we conservatively restrict the designation 'expressed anterior to the MF' to probes where this is seen for >50% of discs, which has never been seen for a sense probe. 7/21 probes labeled anterior to the MF by this criterion. The seven genes for which probes only occasionally detected signal, as well as 1 gene for which no signal was detected (*e.g.*, Figure 4, H), may be expressed anterior to the MF, or their transcripts may fall below the threshold for consistent detection.

A second cluster containing genes expressed in progenitors anterior to the MF

An additional group of progenitor reference genes, *cyclin B3* (*CycB3*), *ey*, *Optix*, *tsh*, and *twin of eyeless* (*toy*), were included in cluster 9 (Figure 1G). Cluster 9 (705 genes) was characterized by gene expression that increased in eye antennal discs from 72-96 h, then decreasing thereafter in eye-antennal discs, eye discs, and antennal discs. Cluster 9 was statistically enriched for 115 GO terms (Supplementary Table S4). Although 20% were related to cell cycle, 42% were related to cellular and organ morphogenesis and metamorphosis, or biological regulation. The top five GO terms were: regulation of biological process, biological regulation, regulation of cellular process, regulation of metabolic process, anatomical structure morphogenesis. The only statistically enriched KEGG pathway was Spliceosome (Supplementary Table S5).

The transcription pattern of genes from cluster 9 was explored by ISH to eye-antennal imaginal discs from third-instar larvae (Figure 4 and Supplementary Figure S5). ISH with probes for 25 genes from cluster 9 identified transcripts from 2 genes in a "cell cycle pattern, ahead of the MF and in the SMW (Figure 4I, M), and 8 genes downregulated at the MF in more than 50% of the discs examined (*e.g.*, Figure 4, J,K,L,O, Supplementary Figure S5). Probes for another 9 genes labeled the anterior of the eye disc in a smaller fraction of eye discs (*e.g.*, Figure 4N) and probes for 6 genes detected no determinable pattern (*e.g.*, Figure 4P, Supplementary Figure S5). In comparison to cluster 7, cluster 9 seemed biased toward expression only in progenitors anterior to the MF, with fewer genes also expressed in the SMW, although the number of genes examined is too small for certainty. The eye disc region ahead of the MF may expand initially before the approaching MF curtails growth at later larval stages, consistent with the Cluster 9 expression profile (Wartlick *et al.* 2014; Fried *et al.* 2016).

Although additional adaptive clustering was able to subdivide cluster 2, analogous BIC-SK mean analyses indicated that clusters 7 and 9 were not subdivided. We therefore assessed the robustness of these clusters when minimum gene expression cutoff other than FPKM >0.5 was used. For example, when only genes with FPKM >1.0 were analyzed, the resulting clusters were not simply contained within the clusters obtained from the larger gene number. We defined the cluster 7 and cluster 9 "core" genes as those genes that clustered together regardless of whether cutoffs of FPKM >0.1, 0.5, or 1.0. The 'core' cluster comprised 1636 genes for cluster 7 (Supplementary Table S7), *i.e.*, 93% of the cluster, indicating that cluster 7 is robust. The 'core' of cluster 9 contained only 138 genes (Supplementary Table S7). Therefore cluster 9 seems to be defined less robustly than cluster 7. For comparison, a similar analysis for cluster 2 identified 882 'core' genes, comprising 86% of cluster 2 and largely overlapping with cluster 2A (699 genes in common) (Supplementary Table S7).

Quantification of gene expression patterns

The χ^2 test indicated that expression pattern differences between Clusters were significantly different ($P = 1.3 \times 10^{-6}$). The fractions of genes induced posterior to the MF (27/52, 0/21, 0/25, respectively) was significantly different ($P = 4.0 \times 10^{-6}$), as were the fractions of genes expressed anterior to the MF or in cell-cycle patterns (7/52, 13/21, 10/25, respectively: $P = 0.001$). By contrast, the fractions of the genes for which no consistent expression was detected (18/52, 8/21, 15/25, respectively) were not significantly different ($P = 0.188$).

The conclusion that Cluster 2, and Clusters 7 and 9 contain genes with significantly different expression patterns depends on the sample of genes selected for ISH being unbiased. As noted, an expression threshold of FPKM ≥ 3 was required for ISH. It is possible that more highly expressed genes might be more likely to have developmental expression patterns. Most genes were above the FPKM ≥ 3 threshold, however (Cluster 2: 759/1029; Cluster 7: 1596/1753; Cluster 9: 585/705), and statistically there was no distinction between expression levels for genes with different expression patterns ($P = 0.085$, Kruskal–Wallis test).

Although most genes were picked for ISH without regard to phenotype, some were selected once eye phenotypes were seen in mutants or after RNAi (see sections below and Table 6). In case genes associated with morphological phenotypes were more likely to have specific expression patterns, we repeated the χ^2 test using only data for ISH of genes selected without regard to phenotype, with similar results (Table 6).

We used the ISH results to estimate how many genes may change expression in accord with differentiation. If the genes tested from Cluster 2 were representative, then Cluster 2 could contain $27/52 \times 1029 = \sim 534$ genes whose expression would be detected posterior to the MF by ISH (95% confidence interval 394–674, Table 6), and a further $18/52 \times 1029 = 356$ genes whose expression pattern would be hard to detect by *in situ* and that might include some further genes expressed posterior to the MF. If calculations are based only on ISH results for genes selected without respect to mutant or knockdown phenotype, the estimates are similar (or $21/43 \times 1029 = \sim 503$ and $16/43 \times 1029 = 383$, respectively).

In the same way, we predicted that Cluster 7 could contain $13/21 \times 1753 = 1085$ genes expressed anterior to the MF or in a cell-cycle pattern, and $8/21 \times 1753 = 668$ genes that might have this expression pattern but be hard to detect. For Cluster 9, the comparable estimates are $10/25 \times 705 = 282$ and $15/25 = 423$. If calculations are based only on ISH results for genes selected without respect to mutant or knockdown phenotype, the predictions are similar (for Cluster 7, $9/16 \times 1753 = 986$ genes expressed anterior to the furrow or in a cell cycle pattern, and for Cluster 9, $5/19 \times 705 = 186$).

In the rest of this paper, we will refer to Differentiation Gene Cluster 2, Proliferation Gene Cluster 7, and Progenitor Gene Cluster 9. These designations are preliminary and intended simply to facilitate discussion; expecially the distinction between Proliferation Gene Cluster 7 and Progenitor Gene Cluster 9, which is based on the enrichment for proliferation GO terms only for Proliferation Cluster 7 as well as the different expression profile.

Comparison with earlier RNA-seq studies

Our results add to previous studies of development gene expression in the eye disc in two respects. First, they increase the estimate for the number of genes upregulated with retinal

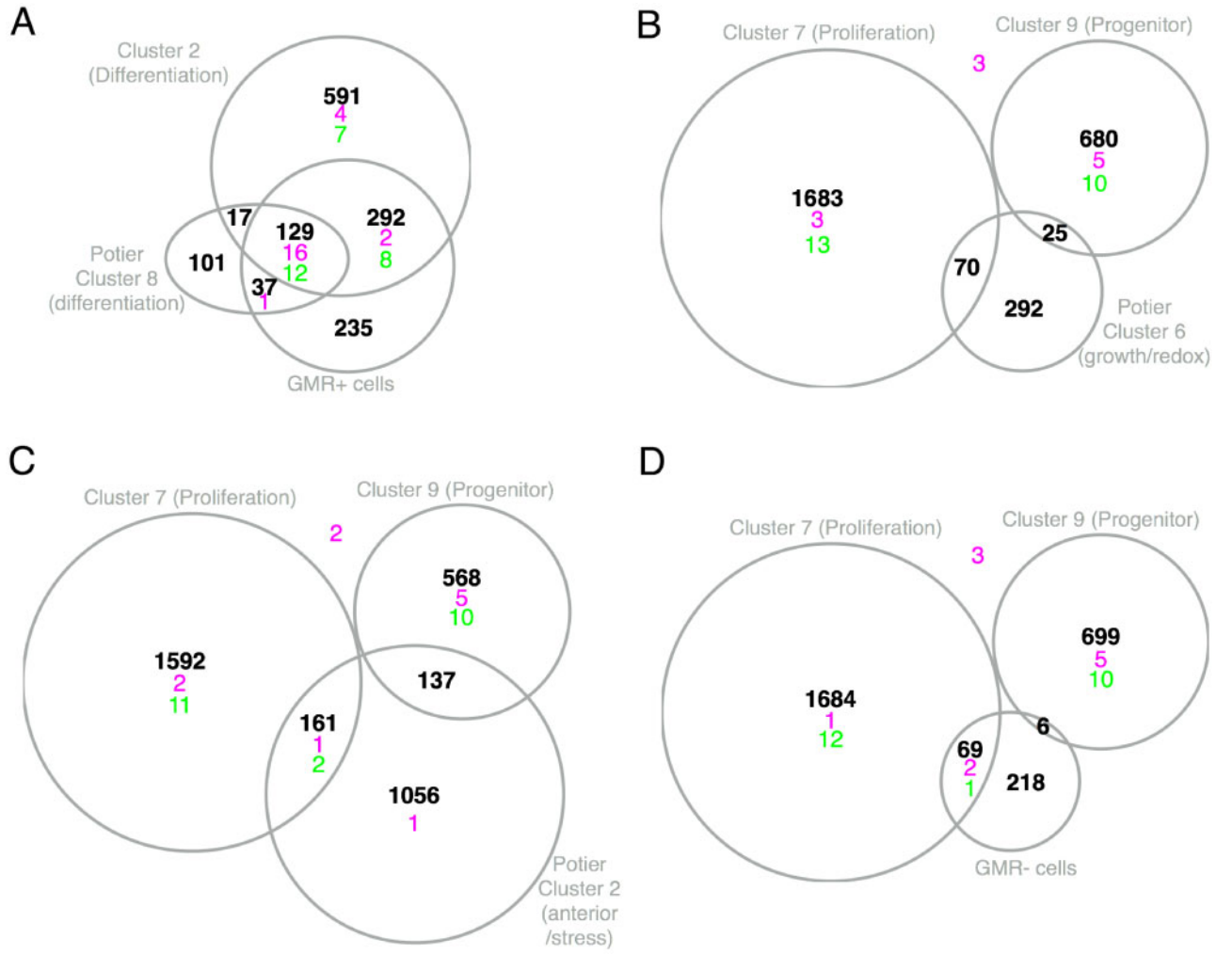

Figure 5 Candidate Differentiation and Progenitor/Proliferation genes compared between studies. Venn diagrams illustrate the correspondence between sets of predicted Differentiation or Proliferation/Progenitor genes predicted from mRNA-Seq of eye-antennal gene expression at different time points (this study) or from different genotypes (Potier et al). Gene numbers are shown in black text. Genes from the reference sets of genes described to be expressed either posterior (A) or anterior to the furrow (B–D) are indicated in magenta. Genes determined in this study to be expressed either posterior (A) or anterior to the furrow (B–D) are indicated in green. (A) The genes predicted to be expressed in differentiating retinal cells by our study, by covariation of gene expression in different genotypes (Potier Cluster 8), or from their enrichment in eye disc cells isolated on the basis of GMR-GAL4 UAS-GFP expression ($P_{Adj} < 0.05$) overlap to roughly similar extents. These overlaps were all much more extensive than expected by chance ($P = 0$, χ^2 test). Although most of the 50 genes for which transcriptional induction posterior to the morphogenetic furrow has been directly shown were predicted by multiple methods, 11 were identified only by our study. (B) The genes we predicted to be expressed in proliferating progenitor cells overlap with a set of genes predicted to be associated with growth and redox by covariation of gene expression in different genotypes (Potier Cluster 6) no more than expected by chance ($P = 0.7843$, χ^2 test; the overlap expected with Proliferation Cluster 7 was 62 genes and with Progenitor Cluster 9 was 25 genes). Potier cluster 6 includes none of the genes now shown to be transcriptionally down-regulated by the morphogenetic furrow. (C) The genes we mapped to Progenitor Cluster 9 overlapped with a set of genes predicted to be associated with anterior eye cells and stress by covariation of gene expression in different genotypes (Potier cluster 2) more than expected by chance (Expected overlap = 88 genes, $P = 2.357E\text{-}08$, χ^2 test). Overlap with genes we mapped to Proliferation Cluster 7 was less than expected, however (Expected overlap = 218 genes, $P = 3.698E\text{-}05$, χ^2 test), and few of the genes shown to be downregulated at the morphogenetic furrow (4/34) were contained within Potier cluster 2. (D). The genes we mapped to Proliferating Cluster 7 overlapped with a set of genes enriched in cells not expressing GFP under GMR-Gal4 control more than expected by chance (Expected overlap = 47 genes, $P = 0.0011422$, χ^2 test), but the genes we mapped to Progenitor Cluster 9 overlapped less (Expected overlap = 19 genes, $P = 0.002499$, χ^2 test). Only 3/34 genes shown to be downregulated by the morphogenetic furrow were among the genes whose expression was enriched in cells lacking GFP expressed under GMR-Gal4 control.

differentiation. Secondly, they identify large groups of genes clearly downregulated upon retinal differentiation.

A previous RNA-seq study also used gene expression clustering to classify results, but compared multiple genotypes rather than multiple timepoints, defining 284 genes predicted to be associated with retinal differentiation posterior to the MF (Potier *et al.* 2014). 51% of these genes fell within the Differentiation Cluster 2 of this study (Figure 5A). In addition, Potier et al dissociated cells expressing GFP posterior to the MF from GMR-Gal4 UAS-GFP eye-antennal imaginal discs. 65% of the genes enriched for expression in GFP+ cells fell within our Differentiation Cluster 2 (Figure 5A). These overlaps are much greater than expected by chance and indicate broad agreement between all three approaches to identify differentiation genes turned on behind the furrow, except that the set of genes up-regulated on eye differentiation is much larger in our study. The 50 genes whose expression posterior to the furrow is shown experimentally (24 selected from previous literature and 26 documented here) were mostly

identified within both our Differentiation Cluster 2 and GMR+ genes, but 11 were exclusive to our Differentiation Cluster 2 (Figure 5A), confirming that our approach has expanded the set of genes upregulated in the differentiating eye disc.

The clusters of genes we found downregulated at the MF had greater novelty. The Potier study tentatively identified gene sets with expression anterior to the MF, as well as with stress (their cluster 2) or associated with growth as well as redox regulation (their cluster 6), without validating expression patterns. These contained only 2 (cluster 2) or none (cluster 6) of the 34 genes whose expression anterior to the furrow is discussed here (11 selected from previous literature and 23 shown in this paper) (Figure 5, B and C). Potier cluster 2 and 6 show only small overlaps with our Proliferation/Progenitor Clusters 7 and 9 and only the overlaps with Potier Cluster 2 are greater than expected by chance (Figure 5, B and C). Potier et al also identified genes whose expression was enriched in eye-antennal imaginal disc cells lacking GMR-driven GFP ie not posterior to the furrow. Only 3 of the 34 genes whose expression anterior to the furrow is documented were included in this set, and overlap with our Proliferation Cluster 7 is modest (Figure 5D). Thus, clustering gene expression temporally, as performed here, seems to have made it possible identify genes that are expressed in proliferating progenitor cells and downregulated at the MF more readily than did previous approaches.

Regulatory motifs associated with proliferation, progenitor, and differentiation genes

To test whether genes sharing similar transcription patterns could be regulated by common transcription factors, genes from each cluster were searched for DNA sequences that might encode response elements. The iCis program identified 55 sequence motifs found in or upstream of Proliferation Cluster 2 genes more than expected by chance. 32 transcription factors were candidates to bind to 21 of these motifs (Supplementary Table S13). There were multiple candidates for some motifs, such as two enriched E-box sequences that may be recognized by any of 10 bHLH proteins. Of those, *ato* and *da* have known functions in larval eye disc differentiation (Jarman *et al.* 1994; Brown *et al.* 1996). Many of the other bHLH proteins have roles in neurogenesis in the antennal disc (as well as in other processes in other tissues such as myogenesis) (Baker and Brown 2018). Motif searches were also performed for subsets of cluster 2 that may be further enriched for genes expressed posterior to the MF, namely cluster 2 A and the cluster 2 core. Some additional motifs were found enriched, including additional E-box sequences that could be targets of Snail and Escargot, transcription factors implicated in the interommatidial pigment cell lattice of the eye (Lim and Tomlinson 2006), in addition to the other bHLH proteins (Supplementary Table S10). A list of all the genes associated with enriched motifs associated with potential transcription factors is shown in Supplementary Table S10.

Importantly, DNA binding proteins from cluster 2 itself had target sites enriched in the cluster 2 genes more than DNA binding proteins from any other cluster. These proteins included *onecut*, *gl*, *sloppy paired 1* (*slp1*), *sloppy paired 2* (*slp2*), *pebbled* (*peb*), *anterior open* (*aop*), *SoxNeuro* (*SoxN*) (Figure 6). Requirements in eye differentiation have already been reported for *onecut*, *gl* and *aop* and a requirement for *SoxN* will be reported below, whereas *slp1* is known to play earlier roles in eye development (Moses *et al.* 1989; Lai and Rubin 1992; O'Neill *et al.* 1994; Flores *et al.* 1998; Maurel-Zaffran and Treisman 2000; Nguyen *et al.* 2000; Sato and Tomlinson 2007; Morrison *et al.* 2018). Taken together, these findings suggest that, to a significant extent the expression of eye differentiation genes posterior to the MF is coordinated by transcription factors with a similar expression pattern.

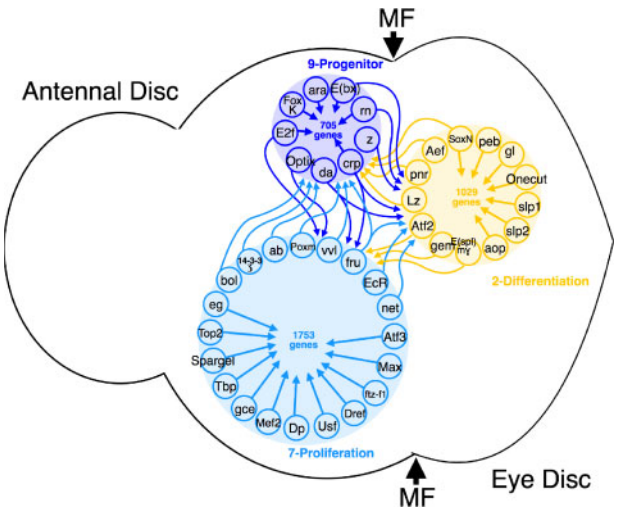

Figure 6 Transcription factors potentially linking differentiation and proliferation genes. Many Transcription Factors (TFs) belonging to gene expression clusters 2, 7, and 9 have cognate recognition motifs that are enriched near Cluster 2, 7, and 9 genes. These include multiple motifs recognized by TFs from the same expression cluster, as well as multiple motifs potentially regulated from the other clusters. Note that in this analysis whether motifs confer positive or negative regulation is not distinguished, and that motifs enriched in Cluster 2A or in the Cluster 2, 7, or 9 cores are included (see text). Motifs potentially recognized by factors mapping in clusters other than 2, 7, and 9 have been omitted. Overall, these motif enrichments suggest that gene expression patterns could be maintained in part by transcription factors with similar expressions themselves. Transcription factors whose binding motifs are enriched among genes with other expression patterns, eg the differentiation gene lz whose motifs are enriched among the Progenitor cluster 9 genes, could be candidates to enforce exclusive gene expression patterns.

Similar observations also held for Clusters 7 and 9. The iCis target analysis found 146 regulatory motifs enriched in the cluster 7 genes, for 110 of which 46 candidate binding proteins could be identified (Supplementary Table S13). Proportionately, cluster 7 itself was the largest source of DNA binding proteins whose target sites were enriched within cluster 7 genes (Figure 6), suggesting that genes encoding transcription factors within cluster 7 [*DNA replication-related element factor* (*Dref*), *Usf*, *Max*, *Activarting Transcription Factor 3* (*Atf3*), *Myocyte enhancer factor 2* (*Mef2*), *Topoisomeras 2* (*Top2*), *eagle* (*eg*), *ftz transcription factor 1* (*ftz-f1*), *Spargel*(*srl*), *DP transcription factor* (*Dp*), *germ cell-expressed bHLH-PAS* (*gce*), *TATA binding protein* (*Tbp*)] coordinate the expression of genes anterior to the MF and during proliferation. Other transcription factor genes were within cluster 9, reflecting the related expression of these clusters (*cropped* (*crp*), da, *E2f*, *Optix*) (Figure 7). The iCis target analysis found 77 regulatory motifs enriched in the cluster 9, for which 28 candidate DNA binding proteins were identified (Supplementary Table S10), many encoded by genes themselves placed in Cluster 9 by expression [*Enhancer of bithorax* (*E(bx)*), *crp*, *rotund* (*rn*), *E2F*, *araucan* (*ara*), *zeste* (z), *Forkhead Box K* (*FoxK*)], whereas other potential regulators of cluster 9 genes were located within cluster 7 (*abrupt* (*ab*), *Pox meso* (*Poxm*), *fruitless* (*fru*), *boule* (bol), *ventral veins lacking* (*vvl*), *14-3-3-zeta*) (Figure 6). Lists of all the genes associated with motifs associated with potential transcription factors and enriched in Clusters 7 and 9 is shown in Supplementary Table S10.

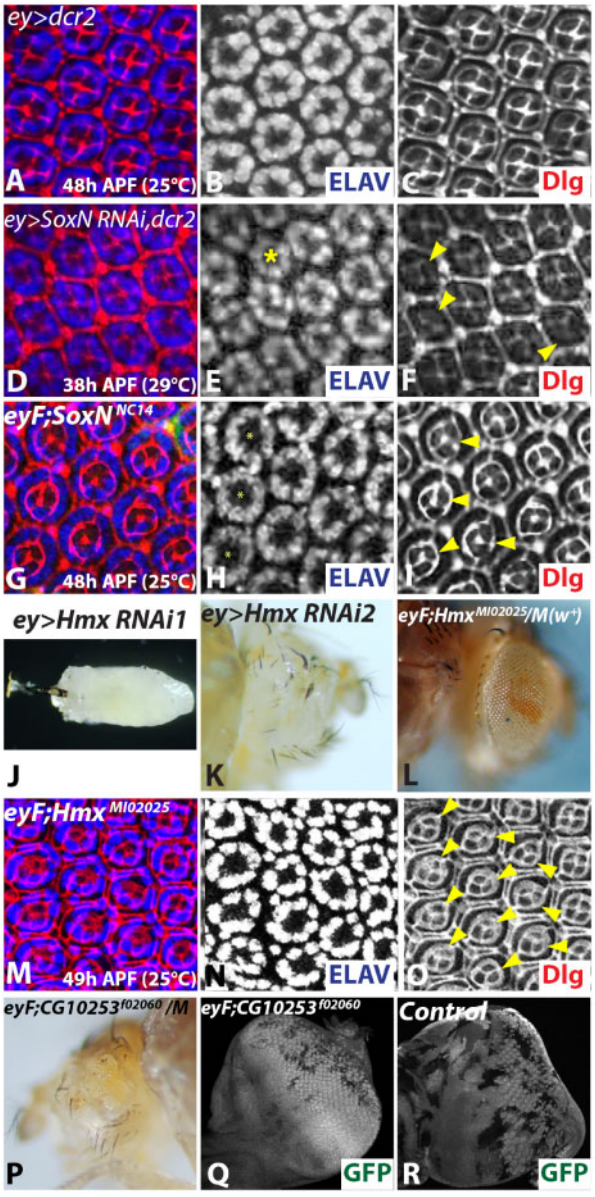

Figure 7 Genes expressed in the differentiating retina are required for eye development. (A–I, M–O) *SoxN* and *Hmx* mutant clones showed cone cell defect phenotypes, (J–L, P–R) *Hmx* knockdowns and *CG10253* mutant clones showed growth defect phenotypes. Adult eyes (K,L,P), pupae (J), eye discs (Q,R) and pupal retinas 38h APF (A–C) or 48-h APF (A–C, G–I, M–O) after being raised at 29°C and 25°C, respectively. ELAV (in blue A, D, G, M) and Dlg (in red in A, D, G) labeled all cell boundaries inside the retina. The focal planes used here clearly distinguished interommatidial cells, the border of each ommatidia unit as well as their four cone cells. Anterior is to the left. Yellow asterisks: ommatidia with a number of photoreceptors different from 8 (E). Yellow arrowheads: ommatidia with a number of cone cells different from 4 (F, I, O). Although RNAi for *SoxN* (D-F) had little effect on neural differentiation in the retina revealed by labeling with anti-ELAV(D–E), the number of non-neuronal cone cells labeled by anti-Cut is reduced from the normal four per ommatidium (F). Homozygosity for a *SoxN* mutation (G–I) induced defects in ommatidia specification with number of photoreceptors different from 8 (H) and number of cone cells different from 4 as shown with the anti-Dlg labeling (I). RNAi for Hmx (J–K) results in the loss of head structures (J) or ablation of the adult eye (K). Homozygosity for an *Hmx* mutation (L–O) leads to a rough appearance of the adult eye (L) and reduction in the number of non-neuronal cone cells (O), although the numbers of retinal neurons appeared normal (N). Homozygosity for a CG10253 mutation (P–R) induced a severe eye phenotype in adult eye (P). Mutant clones did not grow properly in WT background (GFP negative cells in Q) compare to the control (R).

Although these results support the notion that transcription factor expression patterns themselves contribute to maintaining similar expression of many other genes, there were also many exmples of transcription factors that regulate genes in other clusters. Ato and Cut (ct), for example, are expressed during eye differentiation and play important regulatory roles but neither is found in cluster 2. *Ato* is transiently transcribed just anterior and posterior to the MF (Jarman *et al.* 1993; Sun *et al.* 1998), which may explain why it did not cluster with either anteriorly- or posteriorly-expressed eye genes in our analysis. *Ct* expression is induced posterior to the MF but shows independent expression dynamics in the antennal disc that may explain why *cut* did not cluster with other eye differentiation genes.

Many transcription factors from Cluster 2 potentially regulate targets in Clusters 7 or 9 Activating Transcription Factor 1 (Atf2), Gemini (gem), E(spl)mγ-HLH, pannier (pnr), SoxN, peb, Lozenge (lz), Adult Enhancer Factor 1 (Aef1)], and vice versa (Cluster 2 was enriched for potential targets of cluster 7 genes *fru*, *Ecdysone Receptor* (*EcR*), *net*, *Tbp* and Cluster 9 genes *da*, *crp*, *E(bx)*, *rn*, *z*) (Figure 6). In principle, such relationships could enforce alternative expression patternsns, by repressing expression of genes from other clusters. Activatory and repressive interactions cannot be distinguished from motif analysis, however, and many more experiments would be required to test this speculation. In addition, some enriched motifs can be targets of regulatory proteins encoded by other expression clusters, such as *CG33260*, *pangolin* (*pan*), *stripe* (*sr*), *Ecdysone-induced protein 74EF* (*Eip74EF*), *pleiohomeotic* (*pho*), *pleiohomeotic like* (*phol*), *nejire* (*nej*), *longitudinals lacking* (*lola*) that are potential Cluster 2 regulators, *lola*, *Methoprene tolerant* (*Met*), *Chorion Factor 2* (*Cf2*), *TBP Associated Factor* (*Taf1*), *knirps like* (*knrl*), *deadpan* (*dpn*), *broad* (*br*) that encode potential Proliferation Cluster 7 regulators, and *grain* (*grn*), *serpent* (*srp*), *sirtuin 6* (*Sirt6*), *CG33260*, *Sox102F*, *pou domain motif 3* (*pdm3*), *br*, *CG3407*, *poil au dos* (*pad*), *E2F2*, *absent md neurons and olfactory sensilla* (*amos*), *nautilus* (*nau*), *zinc finger protein* (*Zif*), *scute* (*sc*), *achaete* (*ac*), *asense* (*ase*), *lethal of scute* (*l(1)sc*), *runt* (*run*), *HLH106* that encode potential Progenitor Cluster 9 regulators. Post-translational control of transcription factor activity could explain how target gene expression patterns can differ from the cognate transcription factor. Pan is a mediator of wingless signaling whose activity is controlled at the level of protein-protein interactions, Ecdysone Receptor activity is controlled by a steroid hormone not transcription, *lola* has many isoforms with distinct expression patterns (Goeke *et al.* 2003; Niwa and Niwa 2016; Bejsovec 2018).

Very noticeable is the number of potential regulators of cluster 7 genes that were found in cluster 3 (*Jun related antigen* (*Jra*), *knirps* (*kni*), *Eip78C*, *Hormone receptor 4* (*Hr4*), *Hormone receptor 39* (*Hr39*), *Hormone receptor 46* (*Hr46*), *estrogen related receptor* (*ERR*), *Enhancer of spli m8* (*E(spl)m8*), *Mnt*, *E2F2*). In fact cluster 3 was proportionately enriched for candidate transcription factors with target sites in cluster 7 to the same degree as was the case for cluster 7 itself (Figure 6; Supplementary Table S10). The expression profile of cluster 3 was similar to cluster 2 *i.e.*, increasing over time in eye-antennal discs and in eye discs, but differed from cluster 2 by also increasing over time in antenna discs (Figure 1, E and F). Many of the candidate trans-acting factors identified in cluster 3 are hormone-responsive (*Eip78C*, *Hr4*, *Hr39*, *Hr46*, *ERR*), possibly indicating temporal regulation of eye gene expression by systemic mechanisms shared with the antennal primordium.

We also searched for response elements using the Homer program (Supplementary Table S11). This program identified 97 sequence motifs assigned to 67 candidate transcription factors in

Cluster 2. The higher proportion of DNA binding proteins within Differentiation Cluster 2 having target sites enriched in the genes of Differentiation Cluster 2 was replicated in the Homer analysis. A number of the enriched response elements were the same such as *da*, *gl*, *onecut* and *crp*. Since *crp* was a member of cluster 9 this gene could act anterior to the furrow to repress the expression of cluster 2 genes. Some other response elements presenting phenotypes in our functional analysis were only found with Homer, including those for *H6-like Homeobox* (*Hmx*) and *lethal(3)neo38* (*l(3)neo38*) (Supplementary Figure S8).

Functional validation of potential differentiation genes

To determine whether new functional contributions to retinal differentiation could be discovered among Differentiation Cluster 2 genes, we examined available mutants of selected genes, particularly focusing on transcription factors. Cluster 2 includes 75 potential transcription factors (defined by the presence of a DNA binding domain). Of these, 27 were already known to function in eye development (Supplementary Table S12). As a pre-screen, RNAi knockdown was performed for 36 of the remaining 48 transcription factors, as well as 20 other genes expressed posterior to the MF (Supplementary Table S13). We used Eyeless-Gal4 (EyGal4), which drives expression in all the eye disc in early larvae, and from anterior to the furrow posteriorly in late eye discs (Hazelett *et al.* 1998), and GMR-Gal4, which only drives expression posterior to the MF (Supplementary Figure S6) (Freeman 1996), in both cases with UAS-Dcr2 to enhance knockdown. For each of these 56 genes, knock-down using multiple RNAi lines (186 in total) was evaluated for changes in adult eye morphology. Where appropriate, differentiation of photoreceptor neurons and of non-neuronal cone cells was evaluated by antibody labeling of eye imaginal discs to detect the neuronal specific protein Elav and the Cut transcription factor that is expressed in non-neuronal cone cells. Knock-down of 14 of these genes was found to affect eye morphology (Supplementary Figure S6, Table 12). Probable mutant strains were available for four of these genes, and in three cases confirmed the RNAi phenotypes (*SoxN*, *Hmx*, *Crc*), but for *l(3)neo38* the mutant had no morphological phenotype.

We observed a new mutant phenotype for the transcription factor SoxN. This HMG Box protein is expressed posterior to the furrow (Cremazy *et al.* 2001). SoxN plays roles in epidermis and central nervous system development (Overton *et al.* 2002; Bahrampour *et al.* 2017; Rizzo and Bejsovec 2017). *SoxN* eye phenotypes were conveniently quantified in the pupal retina, when the regular retinal organization is apparent and all the cells occupy precise locations (Figure 7, A–C). *SoxN* knockdown sometimes affected the numbers of Elav-expressing photoreceptor neurons (Figure 7, D–F). More consistently, SoxN downregulation reduced the number of cone cells in 83% of ommatidia (Figure 7, D–F). This phenotype was confirmed in a *SoxN* mutant allele (Figure 7, G–I). Therefore, SoxN is a transcription factor induced posterior to the MF that is required for proper specification or maintenance of cone cells as well as some neurons, based on both RNAi and mutant analysis.

A second transcription factor in cluster 2 is the Hmx protein, which is transcribed posterior to the MF (Supplementary Figure S3A). Knocking down Hmx during *Drosophila* eye development resulted in reduction or absence of the adult eye, or failure of head development, the latter associated with pupal lethality (Figure 7, J and K). When we generated clones of *Hmx* homozygous cells, the number and arrangement of photoreceptor neurons was normal, but a shortfall of cone cells was observed, identifying Hmx as a second transcription factor required for proper specification or maintenance of cone cells (Figure 7, M–O). To generate eyes that were entirely mutant for *Hmx* we used eyFlp to stimulate mitotic recombination in *Hmx/RpS3* transheterozygotes, where the *RpS3/RpS3* recombinant genotype is cell lethal (Newsome *et al.* 2000). These eyes had a rough external eye, consistent with cone cell defects. It is also possible that Hmx mutations might affect growth, since we found that the ratio of *Hmx/Rp* cells to *Hmx/Hmx* cells was greater than expected (Figure 7L).

The RNAi phenotype we found for *Crc*, which was reduced or absent head structures, was already reported for *Crc* mutants (Hewes *et al.* 2000). The phenotype seen for multiple RNAi lines targeting *l(3)neo38*, a gene that is also transcribed behind the MF and encodes a Zinc finger C2H2 transcription factor, was not replicated in a mutant (Supplementary Figure S7, P–T).

We also describe a mutant phenotype for the *CG10253* gene, for which RNAi was not performed. *CG10253* encodes the Alkyldihydroxyacetonephosphate synthase protein involved in the biosynthesis of ether phospholipids. *CG10253* gene expression was found posterior to the MF (Supplementary Figure S3A). Attempting to make *CG10253* homozygous eyes using eyFlp recombination in a *CG10253/RpS18* heterozygote greatly reduced the eye, indicating a role in eye progenitor cell growth or in retinal differentiation (Figure 7P). In mosaic eye discs, individual *CG10253* mutant clones grew poorly compared to control clones (Figure 7, Q and R). We did not examine Elav or Cut labeling, since mutant cells were mostly absent.

RNAi phenotypes for which no mutant allele was examined must be considered provisional. An example was *dpr12*, a gene transcribed posterior to the MF, encoding a cell surface protein with immunoglobulin repeats that seems to play a role at the synapse (Kurusu *et al.* 2008; Carillo 2015). Knock-down of *dpr12* using eyGal4 led to a small, rough eye and a smaller eye field in the eye imaginal disc (Supplementary Figure S6G), and defects in photoreceptor and cone cell differentiation and arrangement (not shown). A similar phenotype was observed with RNAi of CG31619, also transcribed posterior to the MF and encoding an immunoglobulin-like protein (Supplementary Figure S6K). RNAi of CG7206 (Supplementary Figure S6I), a PIN domain protein, severely reduced the eye. Knock-down of *dpr12* and *CG31619* in cells posterior to the MF using the GMR-Gal4 driver resulted in a glassy adult eye (Supplementary Table S14). Other genes that gave phenotypes on RNAi that were not validated in mutants or seen with only one RNAi line are listed in the Supplementary Table S14).

Functional validation of potential progenitor and proliferation genes

To assess the function of genes expressed anterior to the MF, mutations in previously uncharacterized DNA-binding proteins were studied (Supplementary Table S12). Significant findings include phenotypes for the *woc*, *Ssrp*, *mxc*, *CG15514*, and *Crp* mutations.

The *woc* gene from Proliferation Cluster 7 was transcribed anterior to the MF (Supplementary Figure S4). Cells homozygous for a *woc* mutation were usually lost from mosaics and the rare mutant clones that survived led to an abnormal adult eye (Figure 8A). To increase the representation of *woc* mutant cells, EyFLP recombination in a *woc/Rp* background was used. This eyFlp genotype was lethal before adulthood, however, an indication that heads comprised mostly of *woc* mutant cells are severely affected. These findings suggest a requirement for *woc* in cell proliferation and survival in the eye antennal imaginal disc.

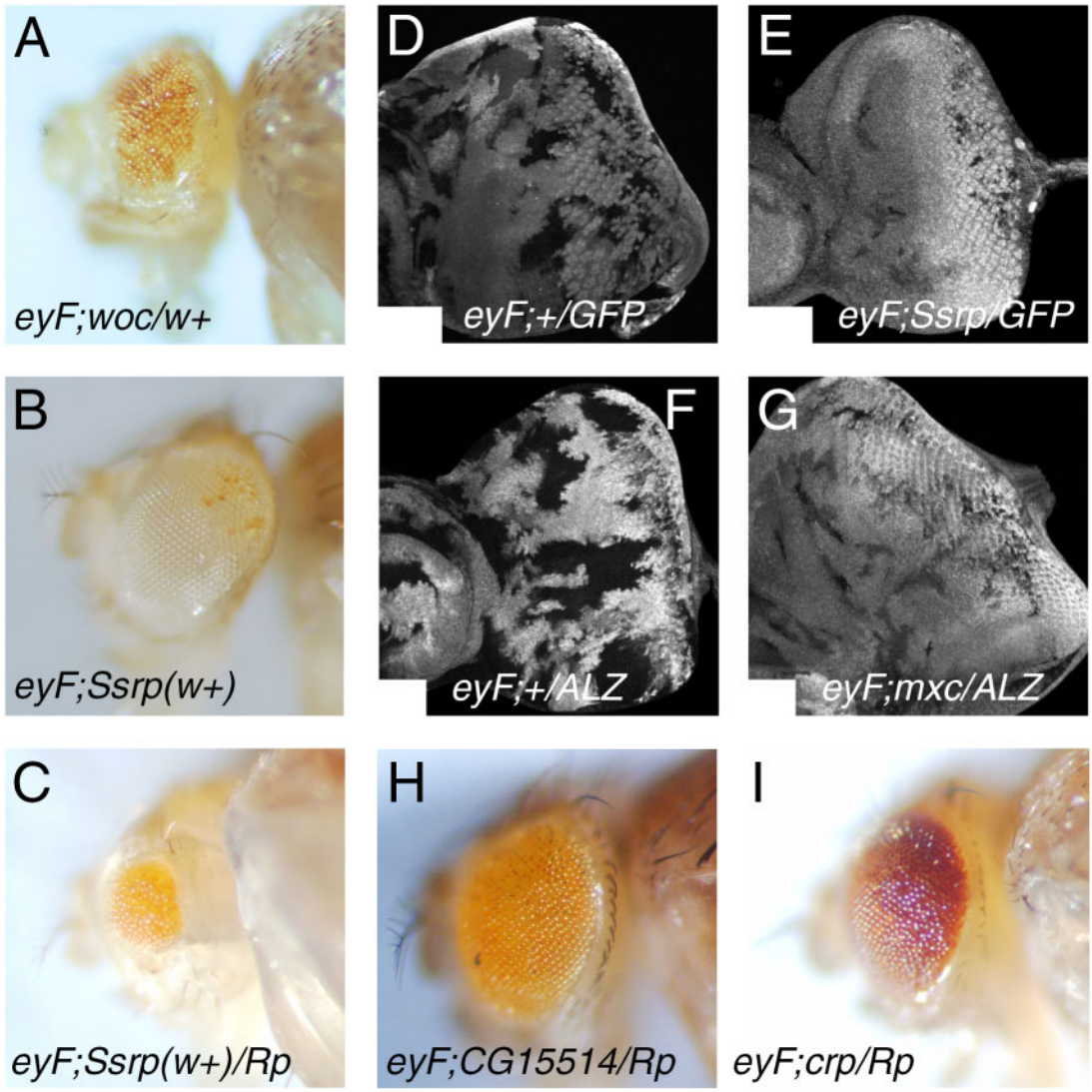

Figure 8 Genes required for growth during eye development. Mosaic clones in adult eyes (A–C, H–I) and eye discs (D–G). (A) When clones of *woc* homozygous mutant cells (unpigmented) are induced in a WT background they produce a small rough eye phenotype indicating a contribution of *woc* to growth. (B) Homozygous *Ssrp* mutant cells (orange) contribute much less to the adult eye than non-mutant cells (white). (C) When growth of non-mutant cells is prevented by a ribosomal protein mutant, the size of the resulting *Ssrp* homozygous eye is reduced considerably. (D) eyFLP recombination leads to colonization of a significant proportion of eye imaginal discs by clones of control cells unlabeled by GFP. (E) By contrast, clones of homozygous *Ssrp* mutant cells are much smaller. (F). eyFLP recombination leads to colonization of a significant proportion of eye imaginal discs by clones of control cells unlabeled by ß-galactosidase. (G) By contrast, clones of homozygous *mxc* mutant cells are much smaller than wild type controls. (H) Eye composed mostly of *CG15514* homozygous cells appeared rough (I) Eye composed mostly of *crp* homozygous cells appeared rough and small.

The *Ssrp* gene from Proliferation Cluster 7 encodes an HMG box protein. The *Ssrp* transcripts were detected in a 'cell cycle' pattern anterior to the MF and in the SMW (Supplementary Figure S4). Homozygous *Ssrp* mutant clones show very little growth compared to wild type clones (Figure 8, B, D, and E). EyFlp recombination of a *Ssrp/Rp* genotype led to a severely reduced eye (Figure 8C). These findings suggest a requirement for *Ssrp* in cell proliferation or survival in the eye antennal imaginal disc.

The *mxc* gene was expressed anterior to the MF (Supplementary Figure S4). Clones of cells mutant for *mxc* showed greatly reduced growth in compared to control wild type clones, consistent with a requirement for growth or survival in the eye antennal imaginal disc (Figure 8, F–G).

CG15514 and Crp, two transcription factors from Progenitor Cluster 9 showed a rough eye phenotype after mitotic clones were induced in a *Rp* mutant background, in which the growth of *CG15514/CG15514* or *crp/crp* mutant clones ought to be enhanced in comparison to the slow-growing *Rp/+* background, suggesting that these genes also affect the proliferative state of cells located anterior to the MF (Figure 8, H–I).

Discussion

Study of *Drosophila* eye development has contributed significantly to the understanding of developmental mechanisms (Cagan 2009; Treisman 2013; Baker and Brown 2018; Kumar 2018). In addition, the tools available for gene expression and knock-down, as well as the fact that eye function is largely dispensable for survival under laboratory conditions, has made the *Drosophila* eye useful for genetic interaction screens whose goal is to understand the function of particular proteins under *in vivo* conditions, including proteins associated with human diseases (Baker *et al.* 2014). Despite this importance, understanding of the particular

transcriptional programs associated with eye cell fate determination and differentiation remains incomplete.

Here we used mRNA-Seq to identify genes whose expression changes temporally over the critical period of eye development where the uncommitted progenitor cells cease dividing, the majority of cell fates are allocated, and terminal differentiation begins with such processes as axon growth and rhodopsin expression. This approach identified gene clusters, respectively, enriched for genes turned on or off as differentiation starts, as verified experimentally by ISH of nearly 100 genes not examined previously.

Differentiation Cluster 2, Proliferation Cluster 7, and Progenitor Cluster 9 contained 3487 genes whose transcripts are temporally regulated during eye differentiation, roughly 1/3 upregulated with time and 2/3 downregulated. ISH of a sample of these estimated that 1901 genes change expression as the MF crosses the eye imaginal disc, ~534 up-regulated and ~ 1367 down-regulated. These may be underestimates because ISH is unable to reveal specific expression patterns below the threshold for detection, and because we have conservatively excluded genes where expression was detected anterior to the MF only inconsistently. Our set of predicted differentiation genes overlaps with those from previous studies, but is larger, and includes new genes with bona fide expression posterior to the furrow showed here. Some known differentiation regulators are nevertheless not recovered in these gene sets, such as the R8 determination genes *ato* and *senseless* (*sens*) that were recovered instead in cluster 4 and the cone cell determination gene *cut* in cluster 5. Even though expression of these genes in the eye disc is upregulated at the MF, the expected temporal accumulation of transcripts may be complicated because these genes have roles in neurogenesis generally and are expressed in other patterns in antennal discs. The large sets of potential Proliferation and Progenitor genes have mostly not been identified in previous studies, and point to the significant changes in progenitor cell functions that accompany terminal cell cycle arrest and differentiation.

We uncovered previously undescribed roles for SoxN, Hmx, CG10253 and the putative cell surface protein Dpr12 in the development of particular differentiated cell types. SoxN encodes an HMG-domain protein previously implicated in neuroblast development and in the regulation of Wg signaling (Overton *et al.* 2002; Bahrampour *et al.* 2017; Rizzo and Bejsovec 2017). Sox2, the human ortholog, is involved in eye development and Sox2 mutations cause the syndromic microphthalmia-3, characterized by small or missing eyes (Fantes *et al.*, 2003). Hmx encodes a homeodomain protein expressed during brain and nervous system development. Homologous mammalian Hmx2 and Hmx3 proteins function in the inner ear and hypothalamus (Wang *et al.* 2004), and their mutations are responsible of the oculoauricular syndrome in human (Gillespie *et al.*, 2015). CG10253 encodes the Alkyldihydroxyacetonephosphate synthase protein involved in the biosynthesis of ether phospholipids. Mutation in the human ortholog causes Rhizomelic chondrodysplasia punctata, type 3, a peroxisomal disorder characterized by congenital cataracts among other symptoms (de Vet *et al.* 1998). Dpr12 encodes a member of a class of transmembrane IgG repeat and LRR proteins implicated in synaptic connectivity but has no precise human ortholog (Carrillo *et al.* 2015).

We found these new morphological phenotypes of transcription factors despite the depth of prior studies of eye development, in which 27 of 75 potential transcription factors in Differentiation Cluster 2 already had known morphological eye phenotypes. Other TF might have functions in eye development that were missed because RNAi was not effective. It is also likely, however, that some transcription factors have redundant functions, or importance for the physiology and function of retinal cells that is not revealed through defects in fate specification during development. For example Pph13, a homeodomain transcription factor found within Differentition Cluster 2, regulates opsin expression and rhabdomere morphogenesis and its mutant phenotype would not have been detected in our morphological assays (Liang *et al.* 2016; Bernardo-Garcia *et al.* 2017). It is a potential strength of expression-based analysis to identify genes whose functional roles are cryptic due to phenotypic subtlety or to redundancy, and some of the remaining transcription factors and other genes expressed posterior to the furrow may fall into this category.

We also verified growth or proliferation phenotypes for mutations of some Cluster 7 or 9 transcription factors *e.g.*, *woc*, *Ssrp*, *mxc*, and potentially *CG15514* and *Crp*. The *woc* gene encodes a zinc finger protein implicated in telomere maintenance (Raffa *et al.* 2005). *Ssrp* encodes an HMG box protein and a RNAi knockdown study also suggested a role in eye growth (Koltowska *et al.* 2013). The *mxc* gene encodes a LIS1 homology motif protein involved in the assembly of histone bodies (White *et al.* 2011). CG15514 is a Zinc finger C2H2 transcription factor with no function previously known and that does not seem to be widely conserved. Crp is a Basic helix-loop-helix (bHLH) transcription factors thought to be a downstream effector of Yki in *Drosophila* tumor growth (Atkins *et al.* 2016).

It might be predicted that the transition from proliferating progenitor cells to committed and differentiating retinal cell types would be associated with overall changes in metabolism and signal transduction, as seen in other systems and as hinted by changes in nucleolar size and in Hh signaling (Tu *et al.* 2005; Chen *et al.* 2007; Baker *et al.* 2009; Tudzarova *et al.* 2011; Baker 2013). These were not identified by simple GO term analyses, however, which only revealed enrichment for neural and retinal differentiation terms among genes expressed posterior to the MF, and terms associated with proliferation and DNA synthesis in Proliferation Cluster 7. On the other hand, the KEGG pathways inositol and phosphatidyl inositol were enriched in the Differentiation Cluster 2 genes, whereas the KEGG pathway 'spliceosome' was enriched in the Proliferation Cluster 7. It may be interesting to determine whether splicing and inositol metabolism change during the transition from progenitors to differentiating cells.

The analysis of potential transcription factor binding site motifs suggests that gene expression patterns are maintained in part by transcription factors that are themselves expressed in broadly similar patterns to their target genes. Examples from Differentiation Cluster 2 include onecut, gl, slp1, slp2, peb, aop, and SoxN. Examples consistent with regulation of the progenitor cell state included transcription factors with important known roles in cell proliferation and growth such as Dref, E2f, Dp, Max, and Spargel, whereas Top2 is important for DNA replication, and *gce* encodes a receptor for Juvenile Hormone that promotes larval growth while antagonizing metamorphosis (Hsieh and Brutlag 1980; Jasper *et al.* 2002; Attwooll *et al.* 2004; Bjorklund *et al.* 2006; Tiefenbock *et al.* 2010; Gallant 2013; Jindra *et al.* 2015). Interestingly, *ara* is believed to play a negative role in growth regulation (Barrios *et al.* 2015). Although transcription factor binding motifs are unreliable predictors of direct regulation for individual genes, where confirmation with direct biding studies using ChIP-seq or similar methods would be important, their overall enrichment across sets of hundreds of genes is likely to be significant.

It is of course interesting to understand how such a large-scale switch in gene expression is controlled. Because there are examples of transcription factors from the Differentiation or Proliferation/Progenitor Clusters whose target motifs are enriched in the other clusters, for example E(spl)mγ, a transcriptional repressor from Differentiation Cluster 2 whose binding morifs were enriched in Proliferation Cluster 7, it is possible that such cross-regulation helps maintain alternative gene expression states. Many more experiments would be required to verify such a speculation. Beyond this, the mechanism of the transition between proliferating progenitor cells and differentiating retina was not revealed by analysis of target motifs. This transition must occur downstream of the Dpp and Hh signaling pathways, but the genes whose expression changes with eye differentiation were not enriched for binding motifs of Ci or Mad, the transcription factors directly mediating Hh and Dpp signaling. It is possible that Ci and Mad regulate relative few genes directly, and more genes indirectly through intermediates. Importantly, Dpp and Hh help switch retinal determination genes from Ey and Tsh expression anterior to the MF, to So, Dac and Eya as the furrow arrives (Bessa *et al.* 2002; Firth and Baker 2009). Recent studies suggest that Hh and Dpp signaling may influence the cell cycle through *so* and *eya*, and progenitor cell proliferation through *ey*, *tsh* and *hth*. These transcription factors directly regulate the cell cycle gene *stg/cdc25* as the MF approaches (Lopes and Casares 2015). Perhaps surprisingly, even though *ey, toy, dac* and *tsh* genes were found within Progenitor Cluster 9, and *eya* and *so* in Differentiation Cluster 2, none of Hth, Ey, Toy, or So motifs were enriched among these clusters. Another retinal determination gene in Progenitor Cluster 9, *optix*, has a target motif enriched in the Proliferation Cluster 7 (Figure 6; the Tsh binding motif is not included in the iCis database). Perhaps target motifs for retinal determination genes are not enriched among target genes because much of this regulation is also indirect. For example, motifs recognized by Gl are enriched in Differentiation Cluster 2. Gl is a direct transcriptional target of So (Jusiak *et al.* 2014a, 2014b), and So is in turn regulated by Dpp and Hh (Bessa *et al.* 2002; Firth and Baker 2009) consistent with a chain of regulatory events regulating eye differentiation downstream the initial triggers. Some functions of Glass are themselves mediated indirectly, for example through the Gl target gene Pph13, which regulates opsin expression and photoreceptor morphogenesis (Liang *et al.* 2016; Bernardo-Garcia *et al.* 2017).

Indirect regulation has also been proposed for cell cycle control by retinal determination genes. A Tsh/Hth overexpression genotype that leads to a highly proliferative tumor state activates many cell cycle genes not enriched for Tsh or Hth motifs even though Tsh and Hth must be responsible for this gene expression profile(Neto *et al.* 2017). Those authors concluded that retinal specification genes affect the cell cycle through relatively few direct targets that then establish a regime of enhanced nuclear hormone signaling that is more directly responsible for most of the gene expression leading to tumorigenesis. We also see evidence for nuclear receptor regulation of gene expression, with enrichment of Eip74EF and EcR motifs in cluster 2 or 2A and of many nuclear receptor motifs in the proliferation cluster 7, suggesting sensitivity of a wide range of genes to nuclear receptor transcription factors might also be regulated in normal development.

In summary, these studies identify large sets of genes up- and downregulated at the transition from proliferating, uncommitted eye progenitor cells to differentiating retinal cell types in the *Drosophila* eye. They suggest that each of these gene expression profiles is maintained to some extent by transcription factors that also share these expression profiles. The transition between progenitor and differentiating cell states, shown by prior studies to depend on Dpp and other signaling pathways, and on changing profiles of retinal determination gene expression, may depend on cascades of transcription factors acting sequentially, rather than any single transcriptional switch co-regulating all or most genes.

Acknowledgments

We thank Dachuan Zhang for isolating RNA, Julie Secombe and Andreas Jenny for comments on the manuscript, and the Chinese Academy of Sciences for a Visiting Professor Award to N.E.B. Supported by grants from the National Institutes of Health to NEB (EY021614 and EY028990, from the National Natural Science Foundation of China to JJH (91749205, 91329302 and 312110103916), from the China Ministry of Science and Technology to JDH (2015CB964803 and 2016YFE0108700). Confocal Imaging was performed at the Analytical Imaging Facility, Albert Einstein College of Medicine, supported by NCI cancer center support grant (P30CA013330), using Leica SP2 and SP5 microscopes.

Conflicts of interest

The authors declare no competing interests.

Literature cited

Aerts S, Quan XJ, Claeys A, Naval Sanchez M, Tate P, *et al.* 2010. Robust target gene discovery through transcriptome perturbations and genome-wide enhancer predictions in Drosophila uncovers a regulatory basis for sensory specification. PLoS Biol. 8:e1000435.

Atkins M, Potier D, Romanelli L, Jacobs J, Mach J, *et al.* 2016. An ectopic network of transcription factors regulated by hippo signaling drives growth and invasion of a malignant tumor model. Curr Biol. 26:2101–2113.

Attwooll C, Lazzerini Denchi E, Helin K. 2004. The E2F family: specific functions and overlapping interests. EMBO J. 23:4709–4716.

Avet-Rochex A, Carvajal N, Christoforou CP, Yeung K, Maierbrugger KT, *et al.* 2014. *Unkempt* is negatively regulated by mTOR and uncouples neuronal differentiation from growth control. PLoS Genet. 10:e1004624.

Bahrampour S, Gunnar E, Jonsson C, Ekman H, Thor S. 2017. Neural lineage progression controlled by a temporal proliferation program. Dev Cell. 43:332–348.e4.

Baker NE. 2013. Developmental regulation of nucleolus size during Drosophila eye differentiation. PLoS One. 8:e58266.

Baker NE. 2017. Patterning the eye: a role for the cell cycle? Dev Biol. 430:263–265.

Baker NE, Bhattacharya A, Firth LC. 2009. Regulation of Hh signal transduction as Drosophila eye differentiation progresses. Dev Biol. 335:356–366.

Baker NE, Brown NL. 2018. All in the family: neuronal diversity and proneural bHLH genes. Development. 145:dev159426.

Baker NE, Firth LC. 2011. Retinal determination genes function along with cell-cell signals to regulate Drosophila eye development: examples of multi-layered regulation by master regulators. Bioessays. 33:538–546.

Baker NE, Li K, Quiquand M, Ruggiero R, Wang LH. 2014. Eye development. Methods. 68:252–259.

Baker NE, Yu S, Han D. 1996. Evolution of proneural atonal expression during distinct regulatory phases in the developing *Drosophila* eye. Curr Biol. 6:1290–1301.

Baonza A, Freeman M. 2001. Notch signalling and the initiation of neural development in the *Drosophila* eye. Development. 128: 3889–3898.

Barrios N, Gonzalez-Perez E, Hernandez R, Campuzano S. 2015. The homeodomain iroquois proteins control cell cycle progression and regulate the size of developmental fields. PLoS Genet. 11: e1005463.

Bejsovec A. 2018. Wingless signaling: a genetic journey from morphogenesis to metastasis. Genetics. 208:1311–1336.

Bernardo-Garcia FJ, Fritsch C, Sprecher SG. 2016. The transcription factor Glass links eye field specification with photoreceptor differentiation in Drosophila. Development. 143:1413–1423.

Bernardo-Garcia FJ, Humberg TH, Fritsch C, Sprecher SG. 2017. Successive requirement of Glass and Hazy for photoreceptor specification and maintenance in Drosophila. Fly (Austin). 11: 112–120.

Bessa J, Gebelein B, Pichaud F, Casares F, Mann RS. 2002. Combinatorial control of *Drosophila* eye development by Eyeless, Homothorax, and Teashirt. Genes Dev. 16:2415–2427.

Bjorklund M, Taipale M, Varjosalo M, Saharinen J, Lahdenpera J, *et al.* 2006. Identification of pathways regulating cell size and cell-cycle progression by RNAi. Nature. 439:1009–1013.

Brown NL, Paddock SW, Sattler CA, Cronmiller C, Thomas BJ, *et al.* 1996. *daughterless* is required for *Drosophila* photoreceptor cell determination, eye morphogenesis, and cell cycle progression. Dev Biol. 179:65–78.

Buttitta LA, Katzaroff AJ, Perez CL, de la Cruz A, Edgar BA. 2007. A double-assurance mechanism controls cell cycle exit upon terminal differentiation in Drosophila. Dev Cell. 12:631–643.

Cagan R. 2009. Principles of Drosophila eye differentiation. Curr Top Dev Biol. 89:115–135.

Carrillo RA, Ozkan E, Menon KP, Nagarkar-Jaiswal S, Lee PT, *et al.* 2015. Control of synaptic connectivity by a network of Drosophila IgSF cell surface proteins. Cell. 163:1770–1782.

Chen Z, Odstrcil EA, Tu BP, McKnight SL. 2007. Restriction of DNA replication to the reductive phase of the metabolic cycle protects genome integrity. Science. 316:1916–1919.

Cremazy F, Berta P, Girard F. 2001. Genome-wide analysis of Sox genes in Drosophila melanogaster. Mech Dev. 109:371–375.

Curtiss J, Halder G, Mlodzik M. 2002. Selector and signalling molecules cooperate in organ patterning. Nat Cell Biol. 4:E48–E51.

Curtiss J, Mlodzik M. 2000. Morphogenetic furrow initiation and progression during eye development in Drosophila: the roles of *decapentaplegic*, *hedgehog* and *eyes absent*. Development. 127: 1325–1336.

Davis TL, Rebay I. 2017. Master regulators in development: Views from the Drosophila retinal determination and mammalian pluripotency gene networks. Dev Biol. 421:93–107.

de Vet EC, Ijlst L, Oostheim W, Wanders RJ, van den Bosch H. 1998. Alkyl-dihydroxyacetonephosphate synthase. Fate in peroxisome biogenesis disorders and identification of the point mutation underlying a single enzyme deficiency. J Biol Chem. 273:10296–10301.

Dokucu ME, Zipursky SL, Cagan RL. 1996. Atonal, Rough and the resolution of proneural clusters in the developing *Drosophila* retina. Development. 122:4139–4147.

Fantes J, Ragge NK, Lynch SA, Mcgill NI, Collin JR, *et al.* 2003. Mutations in *SOX2* cause anophthalmia. Nat Genet. **33**:461–463.

Firth LC, Baker NE. 2005. Extracellular signals responsible for spatially regulated proliferation in the differentiating Drosophila eye. Dev Cell. 8:541–551.

Firth LC, Baker NE. 2007. Spitz from the retina regulates genes transcribed in the second mitotic wave, peripodial epithelium, glia and plasmatocytes of the Drosophila eye imaginal disc. Dev Biol. 307:521–538.

Firth LC, Baker NE. 2009. Retinal determination genes as targets and possible effectors of extracellular signals. Dev Biol. 327:366–375.

Flores GV, Daga A, Kalhor HR, Banerjee U. 1998. Lozenge is expressed in pluripotent precursor cells and patterns multiple cell types in the Drosophila eye through the control of cell-specific transcription factors. Development. 125:3681–3687.

Freeman M. 1996. Reiterative use of the EGF receptor triggers differentiation of all cell types in the *Drosophila* eye. Cell. 87:651–660.

Fried P, Sanchez-Aragon M, Aguilar-Hidalgo D, Lehtinen B, Casares F, *et al.* 2016. A model of the spatio-temporal dynamics of Drosophila eye disc development. PLoS Comput Biol. 12:e1005052.

Fu W, Baker NE. 2003. Deciphering synergistic and redundant roles of *Hedgehog*, *Decapentaplegic* and *Delta* that drive the wave of differentiation in Drosophila eye development. Development. 130: 5229–5239.

Fu W, Noll M. 1997. The Pax2 homolog *sparkling* is required for development of cone and pigment cells in the Drosophila eye. Genes Dev. 11:2066–2078.

Gallant P. 2013. Myc function in Drosophila. Cold Spring Harb Perspect Med. 3:a014324.

Gillespie R L, Urquhart J, Lovell S C, Biswas S, Parry N R A, *et al.* 2015. Abrogation of *HMX1* Function Causes Rare Oculoauricular Syndrome Associated With Congenital Cataract, Anterior Segment Dysgenesis, and Retinal Dystrophy. Investigative Ophthalmology & Visual Science. **56**:883–891.

Goeke S, Greene EA, Grant PK, Gates MA, Crowner D, *et al.* 2003. Alternative splicing of lola generates 19 transcription factors controlling axon guidance in Drosophila. Nat Neurosci. 6:917–924.

Greenwood S, Struhl G. 1999. Progression of the morphogenetic furrow in the *Drosophila* eye: the roles of *Hedgehog*, *Decapentaplegic* and the Raf pathway. Development. 126: 5795–5808.

Hayashi T, Xu C, Carthew RW. 2008. Cell-type-specific transcription of *prospero* is controlled by combinatorial signaling in the Drosophila eye. Development. 135:2787–2796.

Hazelett DJ, Bourouis M, Walldorf U, Treisman JE. 1998. *Decapentaplegic* and *wingless* are regulated by *eyes absent* and *eyegone* and interact to direct the pattern of retinal differentiation in the eye disc. Development. 125:3741–3751.

Heinz S, Benner C, Spann N, Bertolino E, Lin Y C, *et al.* 2010. Simple Combinations of Lineage-Determining Transcription Factors Prime cis-Regulatory Elements Required for Macrophage and B Cell Identities. Molecular Cell. **38**:576–589.

Hewes RS, Schaefer AM, Taghert PH. 2000. The *cryptocephal* gene (ATF4) encodes multiple basic-leucine zipper proteins controlling molting and metamorphosis in Drosophila. Genetics. 155: 1711–1723.

Hsieh T, Brutlag D. 1980. ATP-dependent DNA topoisonmerase from D. melanogaster reversibly catenates duplex DNA rings. Cell. 21: 115–125.

Imrichová H, Hulselmans G, Kalender atak Z, Potier D, Aerts S. 2015. i-cisTarget 2015 update: generalized cis-regulatory enrichment analysis in human, mouse and fly. Nucleic Acids Res. **43**: W57–W64.

Jarman AP, Grau Y, Jan LY, Jan YN. 1993. *atonal* is a proneural gene that directs chordotonal organ formation in the *Drosophila* peripheral nervous system. Cell. 73:1307–1321.

Jarman AP, Grell EH, Ackerman L, Jan LY, Jan YN. 1994. *atonal* is the proneural gene for *Drosophila* photoreceptors. Nature. 369:398–400.

Jasper H, Benes V, Atzberger A, Sauer S, Ansorge W, *et al.* 2002. A genomic switch at the transition from cell proliferation to terminal differentiation in the Drosophila eye. Dev Cell. 3:511–521.

Jin M, Aibar S, Ge Z, Chen R, Aerts S, *et al.* 2016. Identification of novel direct targets of Drosophila Sine oculis and Eyes absent by integration of genome-wide data sets. Dev Biol. 415:157–167.

Jindra M, Uhlirova M, Charles JP, Smykal V, Hill RJ. 2015. Genetic evidence for function of the bHLH-PAS protein Gce/Met as a juvenile hormone receptor. PLoS Genet. 11:e1005394.

Jusiak B, Karandikar UC, Kwak SJ, Wang F, Wang H, *et al.* 2014a. Regulation of Drosophila eye development by the transcription factor Sine oculis. PLoS One. 9:e89695.

Jusiak B, Wang F, Karandikar UC, Kwak SJ, Wang H, *et al.* 2014b. Genome-wide DNA binding pattern of the homeodomain transcription factor Sine oculis (So) in the developing eye of Drosophila melanogaster. Genom Data. 2:153–155.

Kawakami K, Sato S, Ozaki H, Ikeda K. 2000. Six family genes–structure and function as transcription factors and their roles in development. Bioessays. 22:616–626.

Kent D, Bush EW, Hooper JE. 2006. Roadkill attenuates Hedgehog responses through degradation of Cubitus interruptus. Development. 133:2001–2010.

Kim D, Pertea G, Trapnell C, Pimentel H, Kelley R, *et al.* 2013. TopHat2: accurate alignment of transcriptomes in the presence of insertions, deletions and gene fusions. Genome Biol. **14**: R36.

Koltowska K, Apitz H, Stamataki D, Hirst EM, Verkade H, *et al.* 2013. Ssrp1a controls organogenesis by promoting cell cycle progression and RNA synthesis. Development. 140:1912–1918.

Kumar JP. 2018. The fly eye: Through the looking glass. Dev Dyn. 247: 111–123.

Kurusu M, Cording A, Taniguchi M, Menon K, Suzuki E, *et al.* 2008. A screen of cell-surface molecules identifies leucine-rich repeat proteins as key mediators of synaptic target selection. Neuron. **59**:972–985.

Lai ZC, Rubin GM. 1992. Negative control of photoreceptor development in Drosophila by the product of the *yan* gene, an ETS domain protein. Cell. 70:609–620.

Li Y, Baker NE. 2001. Proneural enhancement by Notch overcomes Suppressor-of-Hairless repressor function in the developing *Drosophila* eye. Curr Biol. 11:330–338.

Liang X, Mahato S, Hemmerich C, Zelhof AC. 2016. Two temporal functions of Glass: Ommatidium patterning and photoreceptor differentiation. Dev Biol. 414:4–20.

Lim HY, Tomlinson A. 2006. Organization of the peripheral fly eye: the roles of Snail family transcription factors in peripheral retinal apoptosis. Development. 133:3529–3537.

Lim J, Choi KW. 2004. Induction and autoregulation of the anti-proneural gene *Bar* during retinal neurogenesis in Drosophila. Development. 131:5573–5580.

Lopes CS, Casares F. 2015. Eye selector logic for a coordinated cell cycle exit. PLoS Genet. 11:e1004981.

Mann RS, Carroll SB. 2002. Molecular mechanisms of selector gene function and evolution. Curr Opin Genet Dev. 12:592–600.

Mao Y, Kerr M, Freeman M. 2008. Modulation of Drosophila retinal epithelial integrity by the adhesion proteins capricious and tartan. PLoS One. 3:e1827.

Maurel-Zaffran C, Treisman JE. 2000. *pannier* acts upstream of *wingless* to direct dorsal eye disc development in Drosophila. Development. 127:1007–1016.

Morrison CA, Chen H, Cook T, Brown S, Treisman JE. 2018. Glass promotes the differentiation of neuronal and non-neuronal cell types in the Drosophila eye. PLoS Genet. 14:e1007173.

Moses K, Ellis MC, Rubin GM. 1989. The *glass* gene encodes a zinc-finger protein required by *Drosophila* photoreceptor cells. Nature. 340:531–536.

Nagaraj R, Banerjee U. 2004. The little R cell that could. Int J Dev Biol. 48:755–760.

Naval-Sanchez M, Potier D, Haagen L, Sanchez M, Munck S, *et al.* 2013. Comparative motif discovery combined with comparative transcriptomics yields accurate targetome and enhancer predictions. Genome Res. 23:74–88.

Neto M, Naval-Sanchez M, Potier D, Pereira PS, Geerts D, *et al.* 2017. Nuclear receptors connect progenitor transcription factors to. Sci Rep. 7:4845.

Newsome TP, Asling B, Dickson BJ. 2000. Analysis of *Drosophila* photoreceptor axon guidance in eye-specific mosaics. Development. 127:851–860.

Nguyen DN, Rohrbaugh M, Lai Z. 2000. The Drosophila homolog of Onecut homeodomain proteins is a neural-specific transcriptional activator with a potential role in regulating neural differentiation. Mech Dev. 97:57–72.

Niwa YS, Niwa R. 2016. Transcriptional regulation of insect steroid hormone biosynthesis and its role in controlling timing of molting and metamorphosis. Develop Growth Differ. 58:94–105.

O'Neill EM, Rebay I, Tjian R, Rubin GM. 1994. The activities of two Ets-related transcription factors required for Drosophila eye development are modulated by the Ras/MAPK pathway. Cell. 78: 137–147.

Ou CY, Lin YF, Chen DF, Chien CT. 2002. Distinct protein degradation mechanisms mediated by Cul1 and Cul3 controlling Ci stability in *Drosophila* eye development. Genes Development. 16: 2403–2414.

Overton PM, Meadows LA, Urban J, Russell S. 2002. Evidence for differential and redundant function of the Sox genes *Dichaete* and *SoxN* during CNS development in Drosophila. Development. 129:4219–4228.

Perry M, Konstantinides N, Pinto-Teixeira F, Desplan C. 2017. Generation and evolution of neural cell types and circuits: insights from the Drosophila visual system. Annu Rev Genet. 51: 501–527.

Pichaud F. 2014. Transcriptional regulation of tissue organization and cell morphogenesis: the fly retina as a case study. Dev Biol. 385:168–178.

Potier D, Davie K, Hulselmans G, Naval Sanchez M, Haagen L, *et al.* 2014. Mapping gene regulatory networks in Drosophila eye development by large-scale transcriptome perturbations and motif inference. Cell Rep. 9:2290–2303.

Quiring R, Walldorf U, Kloter U, Gehring WJ. 1994. Homology of the *eyeless* gene of Drosophila to the *Small eye* gene in mice and Aniridia in humans. Science. 265:785–789.

Raffa GD, Cenci G, Siriaco G, Goldberg ML, Gatti M. 2005. The putative Drosophila transcription factor woc is required to prevent telomeric fusions. Mol Cell. 20:821–831.

Rizzo NP, Bejsovec A. 2017. SoxNeuro and Shavenbaby act cooperatively to shape denticles in the embryonic epidermis of Drosophila. Development. 144:2248–2258.

Roignant J-Y, Treisman JE. 2009. Pattern formation in the Drosophila eye disc. Int J Dev Biol. 53:795–804.

Rubin GM, Chang HC, Karim FD, Laverty T, Michaud NR, *et al.* 1997. Signal transduction downstream from Ras in *Drosophila*. Cold Spring Harbor Symp Quantit Biol. 62:347–352.

Ruggiero R, Kale A, Thomas B, Baker NE. 2012. Mitosis in neurons: Roughex and APC/C maintain cell cycle exit to prevent cytokinetic and axonal defects in Drosophila photoreceptor neurons. PLoS Genet. 8:e1003049.

Sato A, Tomlinson A. 2007. Dorsal-ventral midline signaling in the developing Drosophila eye. Development. 134:659–667.

Sun Y, Jan LY, Jan YN. 1998. Transcriptional regulation of *atonal* during development of the *Drosophila* peripheral nervous system. Development. 125:3731–3740.

Tee AR, Sampson JR, Pal DK, Bateman JM. 2016. The role of mTOR signalling in neurogenesis, insights from tuberous sclerosis complex. Semin Cell Dev Biol. 52:12–20.

Tiefenbock SK, Baltzer C, Egli NA, Frei C. 2010. The Drosophila PGC-1 homologue Spargel coordinates mitochondrial activity to insulin signalling. EMBO J. 29:171–183.

Trapnell C, Hendrickson DG, Sauvageau M, Goff L, Rinn JL, *et al.* 2013. Differential analysis of gene regulation at transcript resolution with RNA-seq. Nat Biotechnol. **31**:46–53.

Treisman JE. 2013. Retinal differentiation in Drosophila. Wires Dev Biol. 2:545–557.

Tu BP, Kudlicki A, Rowicka M, McKnight SL. 2005. Logic of the yeast metabolic cycle: temporal compartmentalization of cellular processes. Science. 310:1152–1158.

Tudzarova S, Colombo SL, Stoeber K, Carcamo S, Williams GH, *et al.* 2011. Two ubiquitin ligases, APC/C-Cdh1 and SKP1-CUL1-F (SCF)-beta-TrCP, sequentially regulate glycolysis during the cell cycle. Proc Natl Acad Sci USA. 108:5278–5283.

Viets K, Eldred K, Johnston RJ. Jr., 2016. Mechanisms of Photoreceptor Patterning in Vertebrates and Invertebrates. Trends Genet. 32:638–659.

Vollmer J, Fried P, Aguilar-Hidalgo D, Sanchez-Aragon M, Iannini A, *et al.* 2017. Growth control in the Drosophila eye disc by the cytokine Unpaired. Development. 144:837–843.

Wang W, Grimmer JF, Van De Water TR, Lufkin T. 2004. *Hmx2* and *Hmx3* homeobox genes direct development of the murine inner ear and hypothalamus and can be functionally replaced by Drosophila Hmx. Dev Cell. 7:439–453.

Wartlick O, Julicher F, Gonzalez-Gaitan M. 2014. Growth control by a moving morphogen gradient during Drosophila eye development. Development. 141:1884–1893.

White AE, Burch BD, Yang XC, Gasdaska PY, Dominski Z, *et al.* 2011. Drosophila histone locus bodies form by hierarchical recruitment of components. J Cell Biol. 193:677–694.

Wolff T, Ready DF. 1993. Pattern formation in the *Drosophila* retina. In: M, Bate, A, Martinez, editors. The Development of Drosophila Melanogaster. Vol 2. Cold Spring Harbor Laboratory Press. p. 1277–1325.

Zhang Q, Zhang L, Wang B, Ou CY, Chien CT, *et al.* 2006. A hedgehog-induced BTB protein modulates hedgehog signaling by degrading Ci/Gli transcription factor. Dev Cell. 10:719–729.

Zhang W, Liu Y, Sun N, Wang D, Boyd-Kirkup J, Dou X, *et al.* 2013. Integrating genomic, epigenomic, and transcriptomic features reveals modular signatures underlying poor prognosis in ovarian cancer. Cell Rep. 4:542–553.

Communicating editor: P. Geyer